Pergamon

Bioorganic & Medicinal Chemistry 8 (2000) 1451–1466

BIOORGANIC & MEDICINAL CHEMISTRY

# Identification of New Cdc25 Dual Specificity Phosphatase Inhibitors in a Targeted Small Molecule Array

Alexander P. Ducruet,[a] Robert L. Rice,[a] Kenji Tamura,[a] Fumiaki Yokokawa,[b] Shiho Yokokawa,[b] Peter Wipf [b] and John S. Lazo[a,*]

[a]*Department of Pharmacology, the Combinatorial Chemistry Center and the Molecular Therapeutic/Drug Discovery Program of the University of Pittsburgh Cancer Institute, University of Pittsburgh, Pittsburgh, PA 15261, USA*
[b]*Department of Chemistry and the Combinatorial Chemistry Center, University of Pittsburgh, Pittsburgh, PA 15260, USA*

Received 23 December 1999; accepted 18 February 2000

**Abstract**—Dual specificity protein phosphatases (DSPases) are key regulators of signal transduction, oncogenesis and the cell cycle. Few potent or specific inhibitors of DSPases, however, are readily available for these pharmacological targets. We have used a combinatorial/parallel synthetic approach to rigidify the variable core region and modify the side chains of 4-(benzyl-(2-[2,5-diphenyl-oxazole-4-carbonyl)-amino]-ethyl)-carbamoyl)-2-decanoylamino butyric acid (or SC-ααδ9), which is the most active element in a previously described library of phosphatase inhibitors (Rice, R. L.; Rusnak, J. M.; Yokokawa, F.; Yokokawa, S.; Messner, D. J.; Boynton, A. L.; Wipf, P.; Lazo, J. S. *Biochemistry* **1997**, *36*, 15965). Several analogues were identified as effective inhibitors of the protein tyrosine phosphatase (PTPase) PTP1B and the DSPases VHR and Cdc25$B_2$. Two compounds, FY3-αα09 and FY21-αα09, were partial competitive inhibitors of Cdc25$B_2$ with $K_i$ values of 7.6±0.5 and 1.6±0.2 μM, respectively. FY21-αα09 possessed only moderate activity against PTP1B. Consistent with its in vitro anti-phosphatase activity, FY21-αα09 inhibited growth in MDA-MB-231 and MCF-7 human breast cancer cell lines. FY21-αα09 also inhibited the $G_2$/M transition in tsFT210 cells, consistent with Cdc25B inhibition. Several architectural requirements for DSPase inhibition were revealed through modification of the side chain moieties or variable core region of the pharmacophore, which resulted in decreased compound potency. The structure of FY21-αα09 provides a useful platform from which additional potent and more highly selective phosphatase inhibitors might be generated. 

## Introduction

Phosphorylation and dephosphorylation by the concomitant actions of kinases and phosphatases are critical control mechanisms for numerous physiological functions.[2] More specifically, protein phosphorylation is the major component of signal transduction pathways, highly regulated processes by which cells convey information from the cell surface to their nucleus or other remote subcellular sites.[3,4] This information then controls such processes as cell growth and differentiation, metabolism, cell cycle regulation, cytoskeletal functions and even transformation.[2,5]

Phosphatases are generally divided into two main groups based on their enzymatic mechanism, structure and substrate specificity. The protein phosphatases (PPases) hydrolyze phosphomonoester bonds found specifically on serine or threonine amino acid residues, while the protein tyrosine phosphatases (PTPases) are phosphotyrosine specific, removing the phosphomonoester from the phosphorylated tyrosine residue, returning it to the analogous initial alcohol.[4,5] A PTPase sub-class is formed by the dual specificity protein phosphatases (DSPases), which are capable of hydrolyzing the phosphomonoester bonds on both phosphotyrosine and phosphoserine/threonine residues found on the same protein substrate.[5] While PTPases have extremely limited sequence similarity, they share the active site signature motif (I/V) HCXAGXGR(S/T)G, harboring the catalytic cysteine residue that plays an essential role in the phosphatase-mediated phosphotyrosine phosphomonoester bond cleavage.[6,7]

The PTPases have diverse biochemical and cellular roles. For example, PTP1B regulates both epidermal growth factor and insulin signaling pathways.[6,8–10]

*Corresponding author. Department of Pharmacology, Biomedical Science Tower E-1340, University of Pittsburgh, Pittsburgh, PA 15261, USA. Tel.: +1-412-648-9319; fax: +1-412-648-2229; e-mail: lazo+@pitt.edu

0968-0896/00/$ - see front matter 
PII: S0968-0896(00)00069-9

PTP1B can also reverse the transformation of cells by v-src, v-crk and v-ras when over-expressed in these cells.[11]

The DSPase VHR (vaccina human-related) regulates mitogenic signaling by specifically dephosphorylating members of the MAPK (mitogen-activated protein kinase) family, namely the extracellular regulated kinases ERK1 and ERK2.[5,12,13] The Cdc25 DSPases coordinate the cell cycle by dephosphorylating, and thereby activating, cell cycle dependent kinases. For example, Cdc25B and Cdc25C dephosphorylate $p34^{cdc2}$ (also known as cdkl) and permit entry into mitosis.[14–17]

Since members of the PTPase family appear to play an important role in cell signaling, cell cycle control and oncogenesis, specific inhibitors of these proteins would be highly desirable. Unfortunately, selective and potent inhibitors of PTPases are not currently available. Present crystallographic data, however, suggest that selective inhibitors may be obtainable as significant differences have been observed in the active site of Cdc25A, VHR and PTP1B phosphatases.[13,14,18] The shallow 6 Å pocket of VHR and the even shallower pocket of Cdc25A can accommodate both phosphotyrosine as well as phosphoserine/threonine residues.[13,14] In contrast, PTP1B possesses a deeper 9 Å catalytic pocket where only the more extended phosphotyrosine side chain, unencumbered by any adjacent phosphoserine/threonine, can reach the nucleophilic cysteine at the base of the catalytic pocket.[5,18] The structural differences present in these phosphatases should be exploitable in the selection of targeted inhibitors. Furthermore, inhibitors may be helpful in biochemically defining other unidentified intracellular functions.

We have used a previously described non-electrophilic phosphatase inhibitor, namely SC-ααδ9,[1] as a pharmacophore to synthesize a new targeted library of small molecules and examined each element for selective DSPase inhibition. Minimal structural changes in the pharmacophore resulted in significant differences in inhibitory properties. In addition, the hydrophobic domain of the core pharmacophore was essential for anti-phosphatase activity. We have defined a structure with enhanced selectivity for the dual specificity phosphatase $Cdc25B_2$. This compound, FY21-αα09, also blocked the proliferation of human breast cancer cells in vitro.

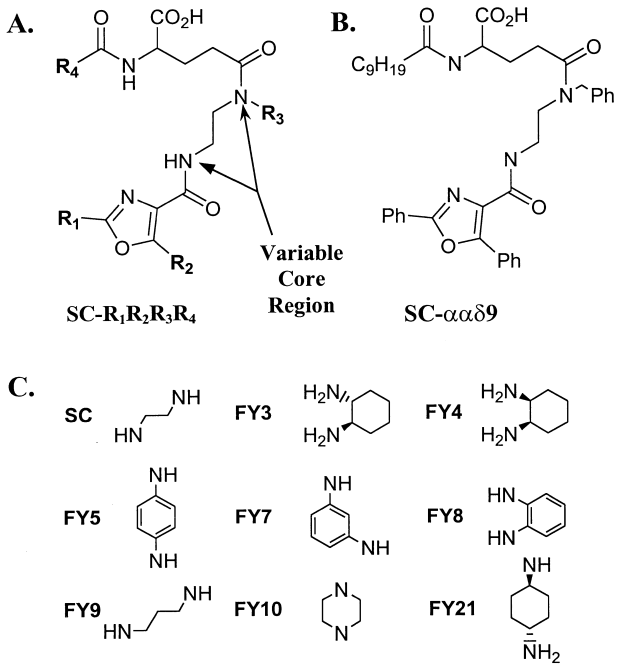


**Figure 1.** SC pharmacophore and variable core region substituents. General chemical structure for the founding SC pharmacophore series. $-R_n$ indicate the combinatorial sites on the pharmacophore and are sequentially listed after the core prefix: (A) the variable core region; (B) chemical structure of SC-ααδ9; (C) structure of variable core diamine linker substitutions.

**Table 1.** Inhibition of $Cdc25B_2$ phosphatase activity and lipophilicity of SC-ααδ9 analogues[a]

| | $Cdc25B_2$ (% Inhibition) | | clog *P* value[b] | |
|---|---|---|---|---|
| Compound | 3 μM | 100 μM | Carboxylate | Free acid |
| (*R*)-SC-ααδ9 | 3±3 | 85±2 | 1.2 | 4.9 |
| (*S*)-SC-ααδ9 | 2±2 | 83±2 | 1.2 | 4.9 |
| SC-ααδA | 6±6 | 78±2 | ND[c] | ND[c] |
| SC-ααδ15 | 11±9 | 76±3 | 3.6 | 8.4 |
| SC-ααδ17A | 13±10 | 78±3 | 4.3 | 8.9 |
| SC-ααδ17B | 7±7 | 79±4 | 4.4 | 9.0 |
| SC-ααδ6III | 7±7 | 13±2 | −2.0 | 1.4 |
| SC-ααδ4II | 6±4 | 23±2 | −1.8 | 1.9 |

[a]Each value is the percent inhibition from untreated control and the mean and SEM from three or more independent determinations.
[b]clog *P* values represent logarithms of the octanol–water partition coefficient and were calculated based on energy-minimized extended conformations by the method of Alkorta and Villar.[26]
[c]ND, not determined.

## Results

### Phosphatase inhibition by SC-ααδ9 enantiomers and $R_4$ analogues

Because we previously found that racemic SC-ααδ9 (Fig. 1B) was an inhibitor of dual specificity phosphatases,[1] we further examined the structural basis for inhibition by synthesizing and testing both the (*R*)-SC-ααδ9 and (*S*)-SC-ααδ9 enantiomers. Both enantiomers inhibited $Cdc25B_2$ phosphatase activity by approximately 85% at 100 μM (Table 1). At 3 μM, neither enantiomers had significant inhibitory activity.

Previous observations lead us to speculate that the hydrophobic nonyl substituent of our SC pharmacophore was critical for phosphatase inhibition.[1] To investigate this hypothesis, we replaced the nonyl moiety ($R_4$) of the SC-ααδ9 core pharmacophore with hydrophobic substituents of variable length (Fig. 2). Compounds such as SC-ααδ15, which contains a pentadecyl side chain, had a greater clog *P* value than SC-ααδ9 but had similar $Cdc25B_2$ inhibitory activity as compared to that seen with SC-ααδ9 (Table 1). Similarly, SC-ααδ17A and SC-ααδl7B, which had greater

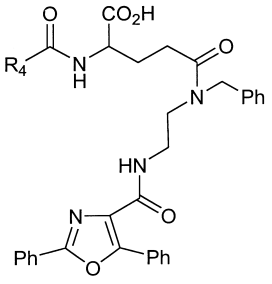

| Compound | $R_4$ |
|---|---|
| SC-ααδ9 | $Me(CH_2)_8$ |
| SC-ααδ15 | $Me(CH_2)_{14}$ |
| SC-ααδ17A | $Me(CH_2)_7CH{=}CH(CH_2)_7$ |
| SC-ααδ17B | $Me(CH_2)_4CH{=}CH{=}CH(CH_2)_7$ |
| SC-ααδA | 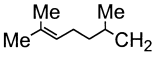 |
| SC-ααδ6III | 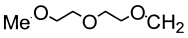 |
| SC-ααδ4II | 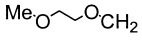 |

**Figure 2.** Chemical structures of SC-ααδ9 $R_4$ analogues.

clog *P* values than SC-ααδ15, maintained anti-$Cdc25B_2$ activity, while the ether-containing SC-ααδ6III and SC-ααδ4II, with the lowest clog *P* values of these compounds, had no inhibitory activity against $Cdc25B_2$ up to a concentration of 100 μM. These results demonstrated a critical role for hydrophobicity rather than just the length of the $R_4$ substituent for $Cdc25B_2$ phosphatase inhibition.

## Phosphatase inhibition by modified core pharmacophore library members

Conformational rigidity can be achieved by replacing the flexible ethyldiamine portion of the original SC-ααδ9 pharmacophore with a series of cyclic diamines (Figs. 1 and 3).

Specifically, cyclohexyldiamine, piperazine and phenyldiamine substructures were used to enhance rigidity of the variable core region and alter overall size. We also examined an extended alkyl linker, a propyldiamine substructure, to determine if the length of the linker was important. Because of the absence of stereospecificity in the parental SC structure, all congeners were synthesized as racemic mixtures. We found SC-ααδ9 > SC-αα09 > SC-α109 as inhibitors of $Cdc25B_2$ (Tables 1 and 2) revealing the importance of an aromatic moiety on the $C_5$ oxazole ($R_2$) position and the $R_3$ amine. The importance of the $R_2$ aromatic moiety was further established with the full FY series, where -αα09 compounds were generally more inhibitory than the -α109 compounds (Table 2). When we examined the inhibition of $Cdc25B_2$ with 100 μM of the -αα09 series, we found that enzyme inhibition was moderately resistant to modification of the core pharmacophore structure (Table 2), although several cores, such as FY9 and FY10, exhibited decreased Cdc25 inhibitory activity. FY21-αα09 was the most effective inhibitor of $Cdc25B_2$ at 3 μM (Table 2), causing a 36% decrease in enzyme activity. In the -α109 series, no compound was as effective as FY21-αα09. Many congeners were similar to SC-α109, although notably, FY3-α109, FY5-α109, FY7-α109 and FY8-α109 exhibited 2- to 5-fold higher inhibitory activity against $Cdc25B_2$ than SC-α109. None of the compounds in the rigidified FY series, however, caused marked inhibition of VHR or PTP1B at 3 μM (Table 2). FY5-αα09 was the only compound with a distinct preference for VHR over $Cdc25B_2$ or PTP1B. FY3-αα09, FY8-αα09 and FY21-αα09 showed no significant in vitro preference for $Cdc25B_2$, VHR or PTP1B in these preliminary studies at 100 μM. A more comprehensive study of FY21-αα09, however, revealed that PTP1B ($IC_{50}$ = 41.4 μM) was approximately 4-fold less sensitive to the compound than $Cdc25B_2$ or VHR ($IC_{50}$s of 7.0 μM and 12.1 μM, respectively) (Fig. 4).

## Inhibition kinetics of compounds

We next determined the kinetic characteristics of $Cdc25B_2$ inhibition with two of our most potent compounds, FY3-αα09 and FY21-αα09. We found that FY3-αα09 and FY21-αα09 were partial competitive inhibitors of $Cdc25B_2$, with $K_i$ values of 7.6±0.5 μM and 1.6±0.2 μM, respectively (Fig. 5). Kinetic studies using 1 to 60 μM FY3-αα09 with VHR and rhPTP1B were most consistent with an S-parabolic noncompetitive inhibition model (data not shown), although higher FY3-αα09 concentrations presented a more mixed profile. The differences in the FY3-αα09 kinetic profiles seen with VHR, PTP1B and $Cdc25B_2$ may reflect the structural dissimilarities of these phosphatases.

## Cell proliferation assays

Previous studies with the founding core library members indicated that only SC-ααδ9 caused marked, concentration-dependent inhibition of tumor cell growth in culture.[19] We found with the current FY series that only FY21-αα09 caused greater than 90% inhibition of MDA-MB-231 cell growth at 100 μM, while 100 μM of either FY8-αα09 or FY21-αα09 inhibited MCF-7 cell growth by greater than 90% (Fig. 6). Studies with tsFT210 cells indicated that a 6 h exposure to 100 μM FY21-αα09 partially blocked cell cycle progression at the $G_2$/M checkpoint while the biochemically inactive congener SC-αα09 did not cause any block (Fig. 7). FY21-αα09 at 100 μM was as effective inhibiting the $G_2$/M transition as the tubulin binder nocodazole at 1 μM. The $G_2$/M block observed with FY21-αα09 is consistent with intracellular inhibition of $Cdc25B_2$.

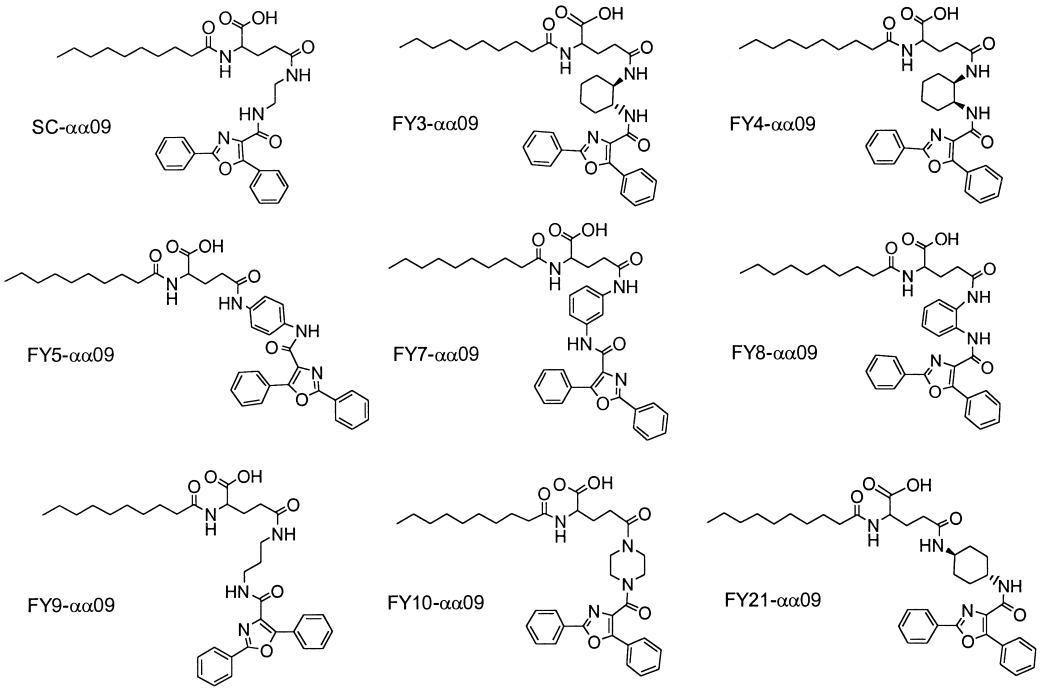


**Figure 3.** Chemical structures of representative analogues of the -αα09 series.

**Table 2.** Inhibition of dual specificity and tyrosine-specific phosphatase activity[a]

| | $Cdc25B_2$ (% inhibition) | | VHR (% inhibition) | | rhPTP1B (% inhibition) | |
|---|---|---|---|---|---|---|
| Compound | 3 μM | 100 μM | 3 μM | 100 μM | 3 μM | 100 μM |
| SC-αα09 | 2.1±1.3 | 57±8.0 | 3.0±0.7 | 6.4±3.6 | −0.2±0.6 | 1.3±2.5 |
| SC-α109 | 2.8±1.7 | 15±7.7 | 4.5±1.4 | 12±1.4 | −0.6±0.7 | −3.5±1.3 |
| FY3-αα09 | 4.0±2.4 | 72±4.4 | 8.4±1.1 | 99± 0.4 | 4.5±1.2 | 89±2.1 |
| FY3-α109 | 3.3±2.3 | 25±9.8 | 5.5±0.3 | 31±1.6 | 4.3±0.7 | 16±1.4 |
| FY4-αα09 | 4.1±2.4 | 73±1.0 | 5.2±0.2 | 61±2.4 | 4.3±1.3 | 33±3.3 |
| FY4-α109 | 1.4±1.0 | 19±7.1 | 1.3±0.3 | 42±0.8 | −0.3±0.2 | 6.7±0.8 |
| FY5-αα09 | 0.9±0.9 | 63±4.3 | 6.4±1.1 | 95±0.9 | 0.7±0.4 | 40±6.3 |
| FY5-α109 | 3.3±3.0 | 48±3.3 | 1.1±2.1 | 65±1.2 | 0.8±0.4 | 23±5.5 |
| FY7-αα09 | 17±4.4 | 80±3.5 | 10±0.5 | 73±3.3 | 1.9±0.8 | 17±1.0 |
| FY7-α109 | 3.1±1.8 | 68±2.7 | 6.4±0.1 | 35±1.2 | 3.1±0.6 | 12±1.3 |
| FY8-αα09 | 4.4±2.8 | 85±2.6 | 6.5±1.0 | 95±1.9 | 5.9±0.9 | 90±2.3 |
| FY8-α109 | 1.1±0.6 | 44±8.8 | 1.7±0.6 | 87±2.4 | 3.8±0.9 | 69±2.4 |
| FY9-αα09 | 0.1±0.1 | 51±5.4 | 2.2±0.9 | 9.0±1.0 | 0.3±0.9 | 3.2±1.4 |
| FY9-α109 | 2.5±4.1 | 4.1±2.4 | 3.4±0.7 | 4.5±2.2 | −0.3±0.5 | −6.3±1.3 |
| FY10-αα09 | 2.3±1.3 | 28±8.3 | 4.4±0.2 | 11±2.7 | −0.4±0.3 | −3.7±1.0 |
| FY10-α109 | 3.2±3.2 | 16±6.9 | 2.6±2.1 | 8.3±3.0 | 0.5±0.3 | −3.8±1.0 |
| FY21-αα09 | 36±1.3 | 83±0.6 | 11±2.7 | 95±2.6 | 3.4±1.6 | 78±1.7 |

[a]Each value is the percent inhibition from untreated control and the mean and SEM from three or more independent determinations.

## Discussion

The dual specificity and tyrosine specific phosphatases share low sequence homology except for conserved residues involved in phosphate binding and catalysis. Based on their crystal structures, Cdc25 and VHR appear to be more accommodating to substrates and less sterically hindered than PTP1B. Our structure–activity relationship results support this conclusion: several of the rigid compounds show marked preference for Cdc25 and VHR rather than PTP1B.

The crystal structure of Cdc25 reveals a hydrophobic region within 20–22 Å of the active site, suggesting that small molecules of a more hydrophobic nature may possess enhanced anti-phosphatase activity.[14] To test the hypothesis that the hydrophobic nonyl substituent in our founding pharmacophore was essential for phosphatase inhibition, we replaced the SC-ααδ9 nonyl moiety, which has an extended length of 22 Å, with various more hydrophobic substituents (Fig. 2). There seemed to be a parallel relationship between clog *P* values and inhibition of $Cdc25B_2$ phosphatase activity. Compounds with $R_4$ substituents of a more hydrophobic nature than the nonyl group found in SC-ααδ9 displayed an inhibitory profile against $Cdc25B_2$ similar to that of SC-ααδ9. On the other hand, compounds with $R_4$ substituents with more hydrophilic character and

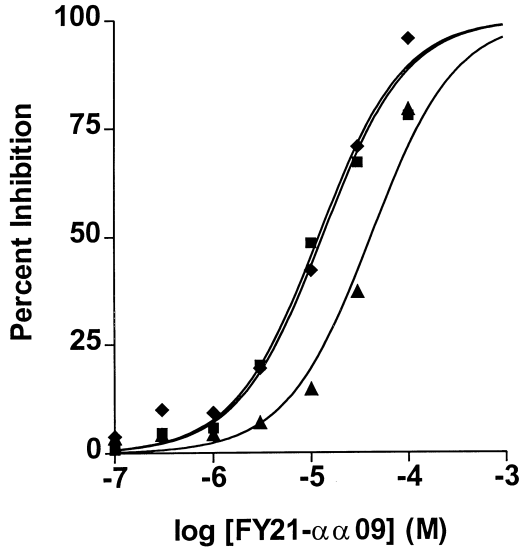


**Figure 4.** Inhibition of dual specificity and tyrosine-specific phosphatases by FY21-αα09. Concentration-dependent phosphatase inhibition by FY21-αα09 (representative results from one experiment). -■-, $Cdc25B_2$; -◆-, VHR; -▲-, PTP1B. Enzyme activities were determined as described in Experimental. Non-linear regressions were performed using GraphPad Prism 3.0.

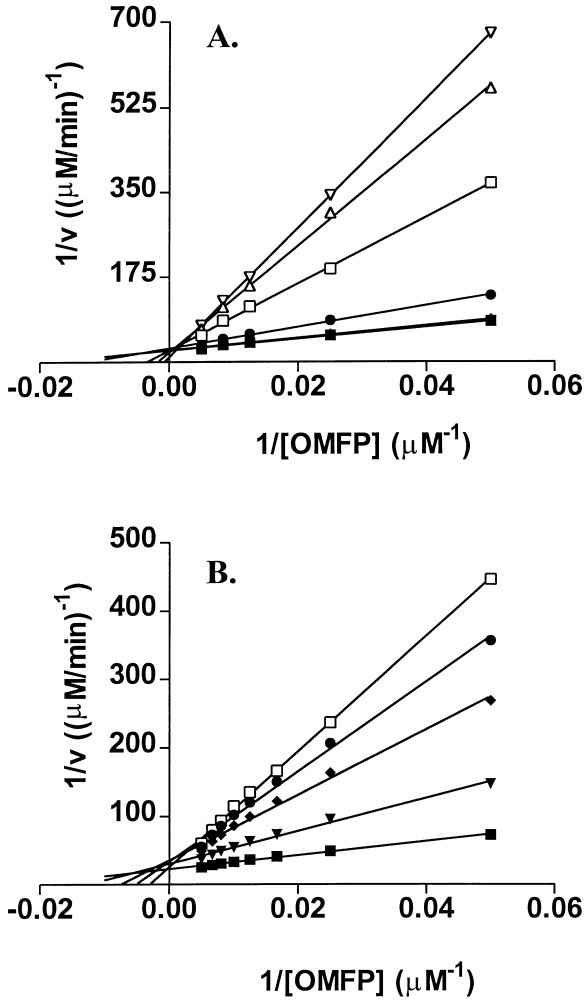


**Figure 5.** Kinetic analysis of $Cdc25B_2$ inhibition by FY3-αα09 and FY21-αα09. Panel A: Lineweaver–Burk plot of $Cdc25B_2$ inhibition by FY3-αα09. -■-, 0 μM; -▼-, 0.1 μM; -●-, 1 μM; -□-, 10 μM -△-, 50 μM; and -▽-, 100 μM FY3-αα09. Panel B: Lineweaver–Burk plot of $Cdc25B_2$ inhibition by FY21-αα09. -■-, 0 μM -▼-, 5 μM; -◆-, 15 μM; -●-, 30 μM; and -□-, 60 μM FY21-αα09. Enzyme activities were determined as described in Experimental procedures and the data fit to the Michaelis–Menten equation. The best fit kinetic model was determined using EZ-Fit™.

therefore lower clog *P* values, such as the ether-containing SC-ααδ6III and SC-ααδ4II, demonstrated negligible $Cdc25B_2$ inhibitory activity at concentrations up to 100 μM. Because kinetic studies with SC-ααδ9 suggest that its mode of inhibition of $Cdc25B_2$ is most consistent with a competitive model, the importance of a hydrophobic moiety in the $R_4$ position of the pharmacophore suggested that the $Cdc2SB_2$ active site, with the exception of the phosphate binding site, is hydrophobic in nature.[1,20]

Rigidification of our basic SC pharmacophore model in our founding targeted array improved the inhibitory profile against DSPases. By replacing the ethyldiamine linker with a cyclohexyldiamine scaffold, such as in FY3-αα09, FY4-αα09 and FY21-αα09, we did not significantly alter the anti-$Cdc25B_2$ activity; these three compounds also efficiently inhibited VHR. FY4-αα09, however, demonstrated significant preference for the DSPases and did not inhibit PTP1B. Perhaps this is due to the less extended nature of FY4-αα09 as compared with the other cyclohexyldiamine congeners. FY21-αα09 was even more potent against DSPases at 100 μM compared with FY4-αα09, but it also inhibited PTP1B; at 3 μM, however, FY21-αα09 displayed a significant preference for $Cdc25B_2$. Perhaps this specificity for $Cdc25B_2$ depends on the previously reported shallow nature of the enzyme's active site relative to that of PTP1B.[14] In addition to rigidifying the pharmacophore, we also varied the substituents at the $R_1$ and $R_2$ positions. All the new compounds with anti-phosphatase activity displayed a strong preference for an aromatic moiety in the $R_2$ position. This may be due to the more hydrophobic nature of DSPase active sites and the documented second aryl phosphate binding site adjacent to the active site of PTP1B.[1,20,21]

In examining a subset of compounds, we found that the better in vitro inhibitors of DSPases were effective inhibitors of breast cancer proliferation. MDA-MB-231 cells were more selective and intrinsically less sensitive to the compounds tested than MCF-7 cells. Cell proliferation was inhibited in a clear concentration response manner, with FY21-αα09 being the most potent agent tested. The growth inhibition seen with several of the compounds, such as FY3-α109, which lacked significant anti-DSPase activity in vitro, seems most likely due to other activities. Cdc25 is the major regulator of the $G_2$/M checkpoint and blockage seen with FY21-αα09 is similar to that observed with other Cdc25 inhibitors.[22] Nonetheless, we recognize that the $G_2$/M block seen with FY21-αα09 could be the result of mechanisms other than inhibition of Cdc25. Additional studies are required to confirm our hypothesis regarding the mechanism of $G_2$/M arrest.

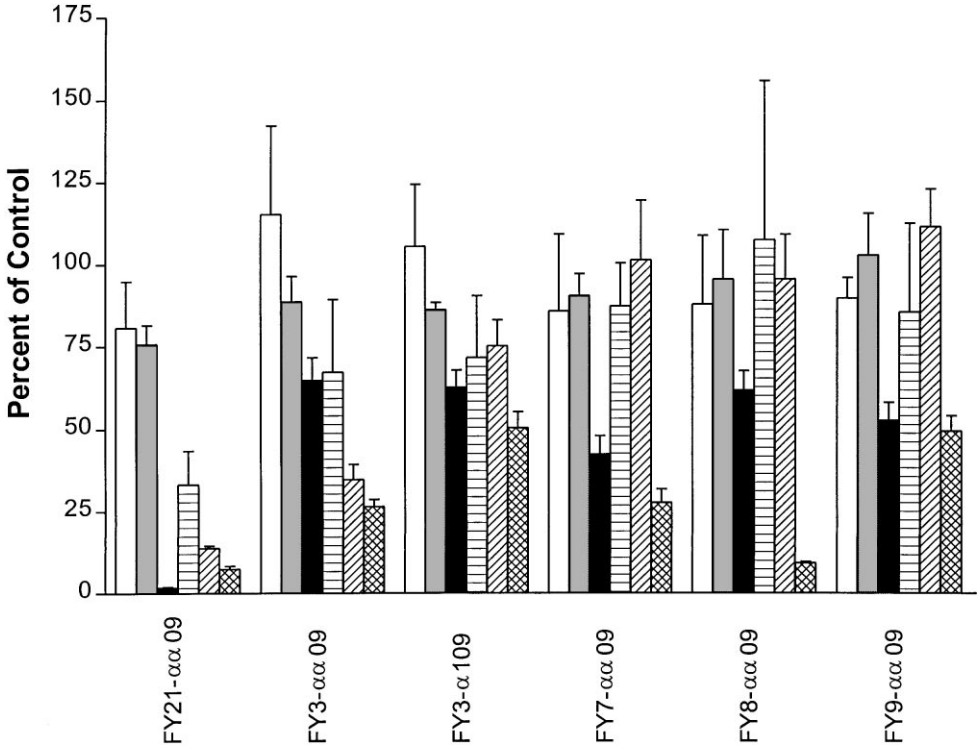


**Figure 6.** Antiproliferative effects of selected compounds on MDA-MB-231 and MCF-7 human breast cancer cells. Antiproliferative effect of compounds. MDA-MB-231 cells: 10 μM (□) 30 μM (▩) and 100 μM (■), MCF-7 cells: 10 μM (▤), 30 μM (▨) and 100 μM (▩). The antiproliferative effect of compounds was determined as described in Experimental procedures and results were normalized to vehicle treated controls. Error bars represent standard deviations ($n = 6$).

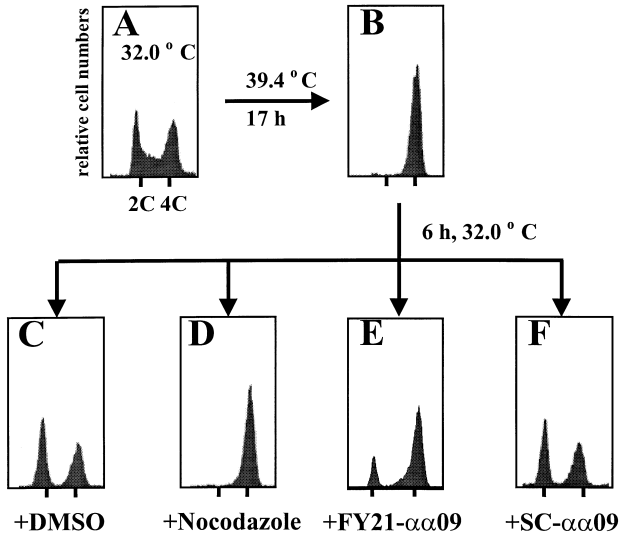


**Figure 7.** Inhibition of tsFT210 cell cycle progression at $G_2$/M by FY21-αα09. (A) tsFT210 cells were cultured at the permissive temperature of 32.0 °C and then (B) incubated for 17 h at the non-permissive temperature of 39.4 °C. Cells were released from cycle arrest by shifting to the 32.0 °C medium. The cells were then incubated for 6 h in the presence of (C) DMSO vehicle, (D) 1 μM nocodazole, (E) 100 μM FY21-αα09 or (F) 100 μM SC-αα09. Fluorescence corresponding to 2C or 4C DNA content is represented by vertical bars.

With FY21-αα09, we have identified one of the most potent $Cdc25B_2$ inhibitors reported to date. Dysidiolide, which was reported to have an $IC_{50}$ of 9.4 μM against Cdc25A,[23] has more recently been found to lack potent inhibitory activity against this phosphatase.[24] A 3-α-azido-B-homo-6-oxa-4-cholesten-7-one derivative had an $IC_{50}$ of 2 μM for Cdc25A, although there is no information concerning its selectivity.[25] Although FY21-αα09 efficiently inhibited both DSPases and PTPases in vitro, unlike SC-ααδ9,[1] it exhibited some preference for the DSPases. As a partial competitive inhibitor, FY21-αα09 interacted with $Cdc25B_2$ in the vicinity of the active site though was unable to completely impede substrate binding. $R_4$ substituents in the original SC pharmacophore revealed the importance of a hydrophobic moiety for $Cdc25B_2$ inhibition and rigidification of the variable core region, and modification of the side chain moieties of the pharmacophore suggests several structural requirements for DSPase inhibition. The structures of FY5-αα09, FY7-αα09 and FY21-αα09 should provide excellent platforms for future analogue development. Our results indicate that selective inhibition of DSPases and PTPases is indeed possible.

## Experimental

### Chemical compounds

We have previously described the general nomenclature system used for our phosphatase library elements.[1] The alphanumeric prefix provides a unique indicator of the core pharmacophore. Thus, the 'SC' prefix was used to designate the pharmacophore used in the founding

phosphatase inhibitor library (Fig. 1A). Replacement of the ethylenediamine in the founding pharmacophore with a *trans* cyclohexyl-1,2-diamine produced the FY3 series, *cis* cyclohexyl-1,2-diamine produced the FY4 series, *para*-phenyldiamine produced the FY5 series, *meta*-phenyldiamine produced the FY7 series, *ortho*-phenyldiamine produced the FY8 series, propyldiamine produced the FY9 series, piperazine produced the FY10 series and a *trans* cyclohexyl-1,4-diamine produced the FY21 series. The FY6 series utilizes ethylenediamine as the core structure. The four descriptors following the prefix indicate the chemical nature of the substituents on the four variable domains of the pharmacophore. The first descriptor always described the substituent ($R_1$) furthest from the assumed surrogate phosphate, a carbonyl moiety in both the SC and FY families. Greek letters indicate an aromatic moiety so that the addition of a phenyl was termed α, a phenethyl was β, benzyl was δ and a styryl was γ.[1] Alkyl chains were designated on the basis of carbon length with Roman numerals and capital letters added if there was chain branching or the inclusion of non-carbon-based linkers. Thus, each compound has a unique name. For most compounds in this study the $R_3$ site was protonated and this was designated as 0. Compounds were resuspended in DMSO prior to use and stocks (powder and resuspended) were stored at −20 °C.

The general synthesis of compounds SC-ααδ9 and SC-αα09 has been previously described.[19] A slightly modified strategy was used for the synthesis of the new compounds SC-ααδ4II and SC-ααδ6III. DL-Glutamate (**1**) was selectively side-chain esterified with trimethylsilyl chloride in allyl alcohol, *N*-protected with β,β,β-trichloroethoxycarbonyl chloride, and methylated to give Troc-Glu(allyl)-OMe (**2b**) in 49% overall yield (Scheme 1). After Pd(0)-catalyzed deallylation, the side-chain carboxyl terminus was extended by PyBroP-mediated coupling with $BnNHCH_2CH_2NHAlloc$, renewed Pd(0)-catalyzed deallylation and coupling with the oxazole segment to give **4**. After deprotection of the *N*-terminus with zinc in acetic acid, EDCI-mediated coupling provided SC-ααδ4II and SC-ααδ6II in 5–10% overall yield from DL-glutamate.

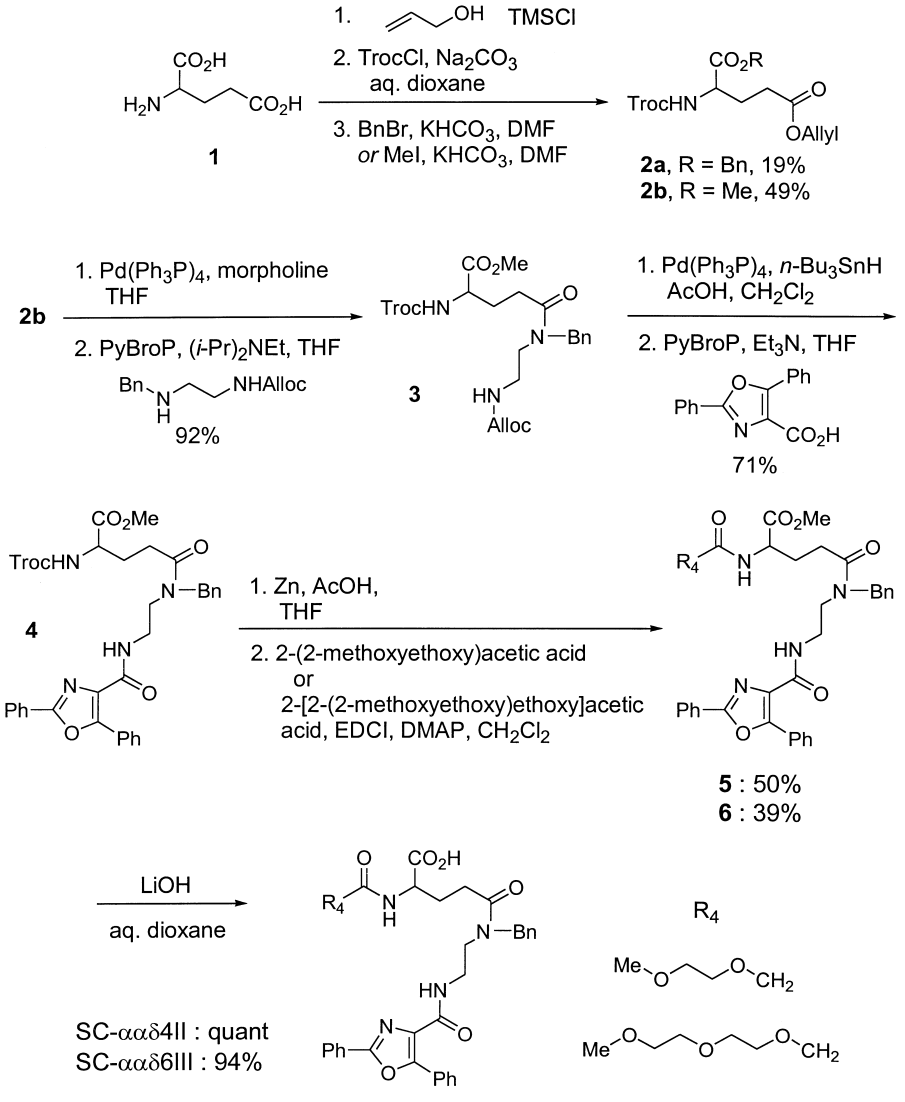


**Scheme 1.**

For the synthesis of FY21-αα09, protected glutamate **2a** was acylated at the *N*-terminus after removal of the Troc group, deallylated and coupled to diamine **8** to give the segment **9** in 52% yield from **2a** (Scheme 2). Acidolytic cleavage of the Boc group and PyBroP-mediated coupling with oxazole **10** provided ester **11**, which was readily converted to the desired FY21-αα09.

Detailed experimental protocols for FY21-αα09, FY3-αα09, FY4-αα09, FY5-αα09, FY7-αα09, FY8-αα09, FY9-αα09, FY10-αα09, SC-ααδ17A, SC-ααδ17B, SC-ααδA, SC-ααδ4II, and SC-ααδ6III are listed below.

## FY21-αα09

**2-(2,2,2-Trichloroethoxycarbonylamino)-pentanoic acid 5-allyl ester 1-benzyl ester (2a).** To a stirred suspension of 10 g (68 mmol) of D,L-glutamic acid (**1**) in 170 mL of allyl alcohol was added dropwise 21.6 mL (170 mmol) of chlorotrimethylsilane. The suspension was stirred at 22 °C for 22 h and concentrated in vacuo. The resulting oil was dissolved in 180 mL of dioxane. The resulting solution was treated with 237.9 mmol of aqueous sodium carbonate (25.21 g in 180 mL of $H_2O$) at 0 °C, stirred for 5 min, and treated with 9.5 mL (69.3 mmol) of TrocCl. The reaction mixture was stirred at 0 °C for 10 min and warmed to 22 °C, stirred for 17 h, concentrated in vacuo, poured into 300 mL of $H_2O$ and washed with $Et_2O$. The aqueous layer was acidified to pH 1 with concentrated HCl, salted out with NaCl, and extracted with EtOAc (3×). The resulting organic layer was dried ($Na_2SO_4$) and concentrated in vacuo to give 8.76 g of carboxylic acid as a yellow oil. To a solution of the resulting oil in 32 mL of DMF was added 3.87 g (38.7 mmol) of $KHCO_3$ and 3.4 mL (29 mmol) of benzyl bromide. The reaction mixture was stirred at 22 °C for 14 h, diluted with EtOAc, and washed with 10% HCl, $H_2O$, saturated aqueous $NaHCO_3$ and brine. The organic layer was dried ($Na_2SO_4$), concentrated in vacuo, and chromatographed on $SiO_2$ (hexanes:EtOAc, 6:1→5:1→4:1→3:1) to give 5.70 g (19% over three steps) of **2a** as a pale yellow oil: IR (neat) 3344, 2953, 1745, 1519, 1327, 1269, 1203 $cm^{-1}$; $^1H$ NMR ($CDCl_3$) δ 7.31 (m, 5H), 5.94–5.83 (m, 1H), 5.69 (d, 1H, $J=8.1$ Hz), 5.34–5.21 (m, 2H), 5.19 (s, 2H), 4.71 (AB, 2H, $J=11.9$ Hz), 4.57 (d, 2H, $J=4.7$ Hz), 4.51–4.44 (m, 1H), 2.50–2.33 (m, 2H), 2.32–2.24 (m, 1H), 2.10–2.01 (m, 1H); $^{13}C$ NMR ($CDCl_3$) δ 172.2, 171.3, 154.2, 135.0, 131.9, 128.6, 128.3, 118.4, 95.3, 74.5, 67.4, 65.4, 53.5, 29.9, 27.2.

**2-Decanoylamino-pentanedioic acid 5-allyl ester 1-benzyl ester (7).** To a solution of 5.698 g (12.59 mmol) of **2a** in 16.5 mL of acetic acid and 24.7 mL of THF was added 16.455 g (251.73 mmol) of zinc dust. The suspension was stirred at 22 °C for 1 h. The reaction mixture was filtered through a Celite pad and the filtrate was concentrated in vacuo. The resulting residue was diluted with EtOAc and washed with saturated aqueous $NaHCO_3$ and brine. The organic layer was dried ($Na_2SO_4$) and concentrated in vacuo to give 2.68 g

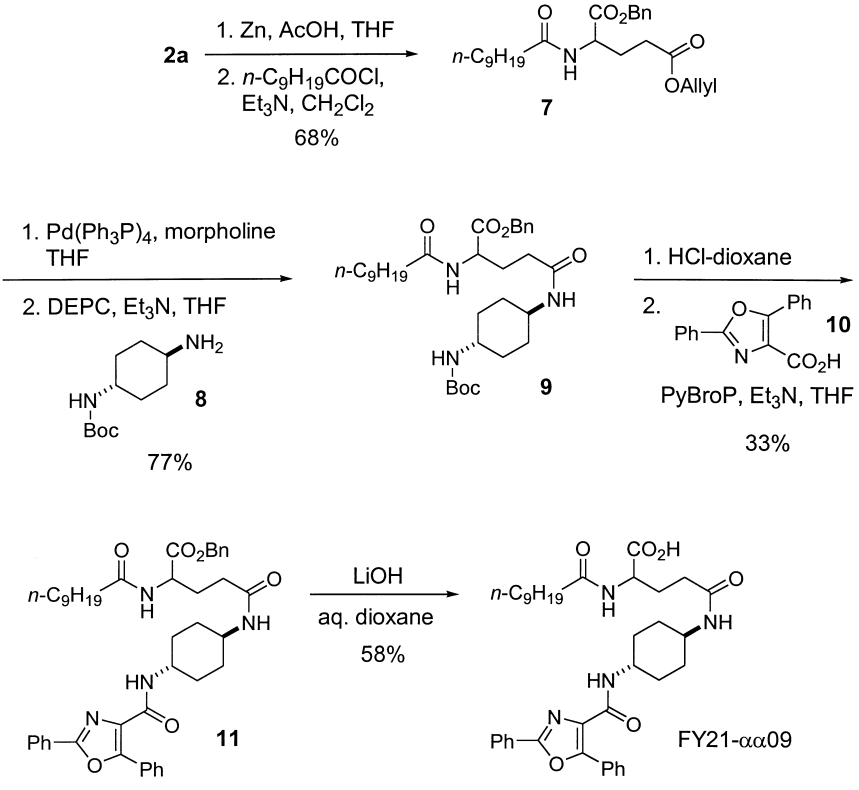


**Scheme 2.**

of free amine. The resulting residue was dissolved in 42 mL of $CH_2Cl_2$ and treated with 5.3 mL (38 mmol) of triethylamine and 3.9 mL (19 mmol) of decanoyl chloride at 0 °C. The reaction mixture was stirred at 0 °C for 15 min and warmed to 22 °C, stirred for 12 h, concentrated in vacuo, diluted with EtOAc, and washed with 10% HCl, $H_2O$, saturated aqueous $NaHCO_3$ and brine. The organic layer was dried ($Na_2SO_4$), concentrated in vacuo, and chromatographed on $SiO_2$ (hexane:EtOAc, 5:1→3:1) to give 3.69 g (68% over two steps) of **9** as a yellow oil: IR (neat) 3293, 3063, 2924, 2855, 1740, 1649, 1534, 1453, 1379, 1175, 986, 930 $cm^{-1}$; $^1H$ NMR δ 7.26 (s, 5H), 6.68 (d, 1H, $J=7.8$ Hz), 5.85–5.75 (m, 1H), 5.22 (d, 1H, $J=17.3$ Hz), 5.14 (d, 1H, $J=10.4$ Hz), 5.08 (s, 2H), 4.63–4.57 (m, 1H), 4.48 (d, 2H, $J=5.6$ Hz), 2.38–2.28 (m, 2H), 2.2–2.1 (m, 3H), 2.0–1.9 (m, 1H), 1.55 (t, 2H, $J=6.9$ Hz), 1.20 (bs, 12H), 0.82 (t, 3H, $J=5.9$ Hz); $^{13}C$ NMR δ 173.0, 172.1, 171.6, 135.0, 131.7, 128.2, 128.1, 127.8, 117.9, 66.8, 64.9, 51.3, 36.0, 31.6, 29.9, 29.1, 29.0, 26.8, 25.3, 22.3, 13.8; MS (EI) *m*/*z* (relative intensity) 431 ($M^+$, 12), 319 (21), 296 (51), 142 (100), 124 (31), 91(91); HRMS (EI) *m*/*z* calcd for $C_{25}H_{37}NO_5$: 431.2672; found: 431.2673.

***trans*-1-Amino-4-*t*-butoxycarbonylamino-cyclohexane (8).** To a solution of 1.0 g (8.8 mmol) of *trans*-1,4-diaminocyclohexane in 30 mL of MeCN was added 1.93 g (8.85 mmol) of $Boc_2O$. The reaction was stirred at 22 °C for 12 h, concentrated in vacuo, poured into 50 mL of $H_2O$, and washed with $Et_2O$. The aqueous layer was acidified to pH 4 with 10% citric acid, salted out with NaCl, and extracted with EtOAc (3×). The resulting organic layer was dried ($Na_2SO_4$) and concentrated in vacuo to give 401 mg (21%) of **8** as a colorless solid: $^1H$ NMR ($CDCI_3$) δ 4.35 (br, 1H), 3.38 (br, 1H), 2.63–2.62 (m, 1H), 2.01–1.97 (m, 2H), 1.87–1.84 (m, 2H), 1.44 (s, 9H), 1.40 (m, 2H), 1.26–1.11 (m, 4H); HRMS (EI) *m*/*z* calcd for $C_7H_{13}N_2O_2$ (M-*t*-Bu): 157.0977; found: 157.0980.

**4-[(*trans*-4-*t*-Butoxycarbonylamino-1-cyclohexyl)-carbamoyl]-2-decanoylamino-butyric acid benzyl ester (9).** To a solution of 518.1 mg (1.201 mmol) of **9** in 8.6 mL of THF was added 1.0 mL (12 mmol) of morpholine followed by 83 mg (0.072 mmol) of tetrakistriphenylphosphine Pd(0) under a nitrogen atmosphere at 22 °C. After stirring for 30 min, the reaction mixture was diluted with EtOAc and washed with 10% HCI and brine. The organic layer was dried ($Na_2SO_4$) and concentrated in vacuo to give 557.2 mg of carboxylic acid as a pale yellow solid. The carboxylic acid (50 mg, 0.13 mmol) and 27 mg (0.13 mmol) of diamine fragment **8** were dissolved in 0.85 mL of THF. To this solution was added 28 μL (0.20 mmol) of triethylamine followed by 25 μL (0.17 mmol) of diethylphosphoryl cyanide (DEPC) at 0 °C. After stirring at 0 °C for 1 h and at 22 °C for 14 h, the reaction mixture was diluted with EtOAc, washed with 10% citric acid, $H_2O$, saturated aqueous $NaHCO_3$ and brine. The organic layer was dried ($Na_2SO_4$), concentrated in vacuo, and chromatographed on $SiO_2$ (hexanes:EtOAc, 1:4→EtOAc) to give 58.2 mg (77%) of **9** as an amorphous solid: $^1H$ NMR ($CDCl_3$) δ 7.35 (br, 5H), 6.54–6.52 (br, 1H), 5.93 (br, 1H), 5.22–5.12 (m, 2H), 4.56 (m, 1H), 4.37 (m, 1H), 3.70 (m, 1H), 3.41 (m, 1H), 2.24–2.17 (m, 5H), 1.19–1.15 (m, 5H), 1.59–1.53 (br, 4H), 1.44 (s, 9H), 1.26 (br, 12H), 0.90–0.86 (m, 5H).

**2-Decanoylamino-4-({5-[2,5-diphenyl-oxazole-4-carbonyl]-*trans*-1,4-cyclohexyl}-carbamoyl)-butyric acid benzyl ester (11).** A mixture of 167 mg (0.284 mmol) of **9** in a HCl/dioxane solution was stirred at 0 °C for 5 min, warmed to 22 °C, stirred for 4 h, and concentrated in vacuo. The resulting residue and 75 mg (0.29 mmol) of oxazole segment **10** were dissolved in 0.95 mL of THF. To this solution was added 99 μl (0.71 mmol) of triethylamine followed by 238 mg (0.511 mmol) of PyBroP at 0 °C. After stirring at 0 °C for 1 h and at 22 °C for 12 h, the reaction mixture was diluted with EtOAc and washed with 10% HCl, $H_2O$, saturated aqueous $NaHCO_3$ and brine. The organic layer was dried ($Na_2SO_4$), concentrated in vacuo, and chromatographed on $SiO_2$ (hexanes:EtOAc, 1:1→1:2→1:3) to give 70 mg (33% over two steps) of **11** as a white solid: $^1H$ NMR ($CDCl_3$) δ 8.38–8.36 (m, 2H), 7.70–7.22 (m, 13H), 5.21–5.10 (m, 2H), 4.54–4.53 (m, 1H), 3.93–3.92 (m, 1H), 3.76 (m, 1H), 2.29–1.82 (m, 8H), 1.61 (br, 2H), 1.47–1.38 (m, 4H), 1.26 (br, 12H), 0.89–0.85 (m, 5H).

**2-Decanoylamino-4-({5-[2,5-diphenyl-oxazole-4-carbonyl]-*trans*-1,4-cyclohexyl}-carbamoyl)-butyric acid (FY21-αα09).** To a solution of 23.6 mg (0.0321 mmol) of **11** in 0.24 mL of dioxane was added 0.385 mmol of aqueous lithium hydroxide (16.2 mg in 0.08 mL of $H_2O$) at 0 °C. The reaction mixture was stirred at 0 °C for 10 min and at 22 °C for 3 h, poured into 20 mL of $H_2O$ and washed with $Et_2O$. The aqueous layer was acidified to pH 1 with 10% HCl, salted out with NaCl, and extracted with EtOAc (3×). The resulting organic layer was dried ($Na_2SO_4$) and concentrated in vacuo to give 12.1 mg (58%) of FY21-αα09 as a pale yellow solid: $^1H$ NMR ($CDCl_3$) δ 7.62–7.19 (m, 10H), 4.26–4.23 (m, 1H), 3.88 (m, 1H), 3.63–3.61 (m, 1H), 2.19–1.76 (m, 19H), 1.55 (m, 2H), 1.41–1.34 (m, 4H), 1.18 (br, 12H), 0.82–0.78 (m, 5H); MS (EI) *m*/*z* 626 ($[M–H_2O]^+$).

## FY3-αα09

**4-[(*trans*-2-*t*-Butoxycarbonylamino-1-cyclohexyl)-carbamoyl]-2-decanoylamino-butyric acid benzyl ester.** According to the procedure described for **9**, **7** (100 mg, 0.255 mmol) was converted to 4-[(*trans*-2-*t*-butoxycarbonylamino-1-cyclohexyl)-carbamoyl]-2-decanoylamino-butyric acid benzyl ester (162 mg, 30%) as an amorphous solid: $^1H$ NMR ($CDCl_3$) δ 7.38–7.28 (m, 5H), 6.91–6.82 (m, 1H), 6.47–6.45 (m, 1H), 5.16–5.11 (m, 2H), 4.74–4.68 (m, 1H), 4.55–4.51 (m, IH), 3.51–3.50 (m, 1H), 3.34–3.31 (m, 1H), 2.24–1.97 (m, 8H), 1.73–1.61 (m, 4H), 1.39 (m, 9H), 1.25 (m, 16H), 0.88 (m, 3H).

**2-Decanoylamino-4-({4-[2,5-diphenyl-oxazole-4-carbonyl]-*trans*-1,2-cyclohexyl}-carbamoyl)-butyric acid benzyl ester.** According to the procedure described for **11**, 4-[(*trans*-2-*t*-butoxycarbonylamino-1-cyclohexyl)-carbamoyl]-2-decanoylamino-butyric acid benzyl ester was converted

to 2-decanoylamino-4-({4-[2,5-diphenyl-oxazole-4-carbonyl]-*trans*-1,2-cyclohexyl}-carbamoyl)-butyric acid benzyl ester (53.8 mg, 78%): $^1$H NMR ($CDCl_3$) δ 8.34–8.32 (m, 2H), 8.11–8.10 (m, 2H), 7.51–7.14 (m, 11H), 6.68–6.57 (m, 1H), 6.41–6.38 (m, 1H), 5.05–4.86 (m, 2H), 4.43–4.36 (m, 1H), 3.81–3.74 (m, 2H), 2.17–1.18 (m, 8H), 1.65–1.32 (m, 8H), 1.24 (br, 12H), 0.87 (m, 3H).

**2-Decanoylamino-44{4-[2,5-diphenyl-oxazole-4-carbonyl]-*trans*-1,2-cyclohexyl}-carbamoyl)-butyric acid (FY3-αα09).** According to the procedure described for FY21-αα09, 2-decanoylamino-4-({4-[2,5-diphenyl-oxazole-4-carbonyl]-*trans*-1,2-cyclohexyl}-carbamoyl)-butyric acid benzyl ester was converted to FY3-αα09 (40.8 mg, 86%): $^1$H NMR ($CDCl_3$) δ 8.30–8.28 (m, 2H), 8.09 (br, 2H), 7.60–7.36 (m, 6H), 4.31 (m, 1H), 3.93 (m, 1H), 3.80 (m, 1H), 2.50–1.83 (m, 8H), 1.52–1.43 (m, 8H), 1.23 (br, 12H), 0.87 (br, 3H); HRMS (EI) *m*/*z* calcd for $C_{37}H_{48}N_4O_6$: 644.3574; found: 644.3595.

## FY4-αα09

**4-[(*cis*-2-*t*-Butoxycarbonylamino-1-cyclohexyl)-carbamoyl]-2-decanoylamino-butyric acid benzyl ester.** According to the procedure described for **9**, **7** (250 mg, 0.637 mmol) was converted to 4-[(*cis*-2-*t*-butoxycarbonylamino-1-cyclohexyl)-carbamoyl]-2-decanoylamino-butyric acid benzyl ester (159 mg, 42%): $^1$H NMR ($CDCl_3$) δ 7.35 (br, 5H), 6.72 (m, 1H), 6.60 (m, 1H), 5.23–5.12 (m, 2H), 4.56 (m, 1H), 4.05 (m, 1H), 3.82 (m, 1H), 2.29–2.18 (m, 4H), 2.02 (m, 2H), 1.70–1.62 (m, 4H), 1.44 (br, 9H), 1.32–1.26 (m, 16H), 0.88 (m, 3H).

**2-Decanoylamino-4-({4-[2,5-diphenyl-oxazole-4-carbonyl]-*cis*-1,2-cyclohexyl}-carbamoyl)-butyric acid benzyl ester.** According to the procedure described for **11**, 4-[(*cis*-2-*t*-butoxycarbonylamino-1-cyclohexyl)-carbamoyl]-2-decanoylamino-butyric acid benzyl ester was converted to 2-decanoylamino-4-({4-[2,5-diphenyl-oxazole-4-carbonyl]-*cis*-1,2-cyclohexyl}-carbamoyl)-butyric acid benzyl ester (41.2 mg, 41%): $^1$H NMR ($CDCl_3$) δ 8.39–8.34 (m, 2H), 8.11–8.02 (m, 2H), 7.52–7.16 (m, 11H), 5.17–4.79 (m, 2H), 4.65–4.56 (m, 1H), 4.36 (1H), 4.16–4.09 (m, 1H), 2.24–1.54 (m, 16H), 1.19 (br, 12H), 0.86 (m, 3H).

**2-Decanoylamino-4-({4-[2,5-diphenyl-oxazole-4-carbonyl]-*cis*-1,2-cyclohexyl}-carbamoyl)-butyric acid (FY4-αα09).** According to the procedure described for FY21-αα09, 2-decanoylamino-4-({4-[2,5-diphenyl-oxazole-4-carbonyl]-*cis*-1,2-cyclohexyl}-carbamoyl)-butyric acid benzyl ester was converted to FY4-αα09 (15.4 mg, quant.) as a pale yellow oil: $^1$H NMR ($CDCl_3$) δ 8.67–8.21 (m, 2H), 8.04–7.98 (m, 2H), 7.45–7.19 (m, 6H), 4.33 (m, 1H), 4.01–3.97 (m, 2H), 2.11–1.47 (m, 16H), 1.16 (m, 12H), 0.78 (m, 3H); MS (EI) *m*/*z* 644 ($M^+$).

## FY5-αα09

**4-[(4-*t*-Butoxycarbonylamino-1-phenyl)-carbamoyl]-2-decanoyl-amino-butyric acid benzyl ester.** According to the procedure described for **9**, **7** (247 mg, 0.631 mmol) was converted to 4-[(4-*t*-butoxycarbonylamino-1-phenyl)-carbamoyl]-2-decanoyl-amino-butyric acid benzyl ester (295 mg, 80%): $^1$H NMR ($CDCl_3$) δ 7.70–7.63 (m, 2H), 7.58–7.30 (m, 7H), 6.48 (m, 2H), 5.21–5.11 (m, 2H), 4.65 (m, 1H), 2.37–2.18 (m, 4H), 1.97 (m, 1H), 1.72 (m, 1H), 1.61 (m, 2H), 1.51 (s, 9H), 1.25 (br. 12H), 0.87 (m, 3H).

**2-Decanoylamino-4-({5-[2,5-diphenyl-oxazole-4-carbonyl]-1,4-phenyl}-carbamoyl)-butyric acid benzyl ester.** According to the procedure described for **11**, 4-[(4-*t*-butoxycarbonylamino-1-phenyl)-carbamoyl}-2-decanoyl-amino-butyric acid benzyl ester was converted to 2-decanoylamino-4-({5-[2,5-diphenyl-oxazole-4-carbonyl]-1,4-phenyl}-carbamoyl)-butyric acid benzyl ester (22.4 mg, 12%) as a pale yellow oil: $^1$H NMR ($CDCl_3$) δ 7.70–7.13 (m, 19H), 5.16 (m, 2H), 4.66 (m, 1H), 2.40–1.81 (m, 6H), 1.61 (m, 2H), 1.25 (br, 12H), 0.87 (m, 3H).

**2-Decanoylamino-4-({5-[2,5-diphenyl-oxazole-4-carbonyl]-1,4-phenyl}-carbamoyl)-butyric acid (FY5-αα09).** According to the procedure described for FY21-αα09, 2-decanoylamino-4-({5-[2,5-diphenyl-oxazole-4-carbonyl]-1,4-phenyl}-carbamoyl)-butyric acid benzyl ester was converted to FY5-αα09 (13.9 mg, 71%): $^1$H NMR ($CDCl_3$) δ 7.62–7.24 (m, 14H), 4.64 (m, 1H), 2.50 (m, 1H), 2.19–1.89 (m, 5H), 1.55 (m, 2H), 1.19 (br, 12H), 0.83 (m, 3H); MS (EI) *m*/*z* 638 ($M^+$), 620 ($[M-H_2O]^+$).

## FY7-αα09

**4-[(3-*t*-Butoxycarbonylamino-1-phenyl)-carbamoyl]-2-decanoyl-amino-butyric acid benzyl ester.** According to the procedure described for **9**, **7** (300 mg, 0.766 mmol) was converted to 4-[(3-*t*-butoxycarbonylamino-1-phenyl)-carbamoyl]-2-decanoyl-amino-butyric acid benzyl ester (194 mg, 43%) as a pale yellow oil: $^1$H NMR ($CDCl_3$) δ 7.64 (br, 1H), 7.34 (br, 5H), 7.20 (m, 3H), 6.70 (m, 1H), 6.58 (m, 1H), 5.20–5.15 (m, 2H), 4.65 (m, 1H), 2.39–2.17 (m, 5H), 2.03 (m, 1H), 1.60 (br, 2H), 1.50 (br 9H), 1.24 (br, 12H), 0.89 (m, 3H).

**2-Decanoylamino-4-({4-[2,5-diphenyl-oxazole-4-carbonyl]-1,3-phenyl}-carbamoyl)-butyric acid benzyl ester.** According to the procedure described for **11**, 4-[(3-*t*-butoxycarbonylamino-1-phenyl)-carbamoyl]-2-decanoyl-amino-butyric acid benzyl ester was converted to 2-decanoylamino-4-({4-[2,5-diphenyl-oxazole-4-carbonyl]-1,3-phenyl}-carbamoyl)-butyric acid benzyl ester (92.7 mg, 79%): $^1$H NMR ($CDCl_3$) δ 8.35 (m, 1H), 8.14–8.02 (m, 2H), 7.52–7.24 (m, 16H), 6.70 (m, 1H), 5.13 (m, 2H), 4.66 (m, 1H), 2.41–1.97 (m, 6H), 1.58 (m, 2H), 1.21 (br, 12H), 0.84 (m, 3H); HRMS (EI) *m*/*z* calcd for $C_{44}H_{48}N_4O_6$: 728.3574; found: 728.3552.

**2-Decanoylamino-4-({4-[2,5-diphenyl-oxazole-4-carbonyl)-1,3-phenyl}-carbamoyl)-butyric acid (FY7-αα09).** According to the procedure described for FY21-αα09, 2-decanoylamino-4-({4-[2,5-diphenyl-oxazole-4-carbonyl]-1,3-phenyl}-carbamoyl)-butyric acid benzyl ester was converted to FY7-αα09 (31.9 mg, quant.): $^1$H NMR ($CDCl_3$) δ 8.24 (m, 1H), 8.04–7.95 (m, 2H), 7.44–7.19 (m, 11H), 4.50 (m, 1H), 2.51–2.44 (m, 2H), 2.20–1.98 (m, 3H), 1.76 (m 1H), 1.50 (m, 2H), 1.12 (br, 12H), 0.76 (m, 3H); MS (EI) *m*/*z* 620 ($[M-H_2O]^+$).

### FY8-αα09

**4-[(2-*t*-Butoxycarbonylamino-1-phenyl)-carbamoyl]-2-decanoyl-amino-butyric acid benzyl ester.** According to the procedure described for **9**, **7** (301 mg, 0.769 mmol) was converted to 4-[(2-*t*-butoxycarbonylamino-1-phenyl)-carbamoyl]-2-decanoyl-amino-butyric acid benzyl ester (239 mg, 53%) as a brown oil: $^1$H NMR ($CDCl_3$) δ 7.57 (m, 1H), 7.48 (m, 1H), 7.34 (br, 5H), 7.19–7.06 (m, 2H), 6.54 (m, 1H), 5.16 (m, 2H), 4.63 (m, 1H), 2.43–2.19 (m, 4H), 2.04–1.82 (m, 2H), 1.60 (m, 2H), 1.49 (br, 9H), 1.25 (br, 12H), 0.88 (m, 3H).

**2-Decanoylamino-4-({3-[2,5-diphenyl-oxazole-4-carbonyl]-1,2-phenyl}-carbamoyl)-butyric acid benzyl ester.** According to the procedure described for **11**, 4-[(2-*t*-butoxycarbonylamino-1-phenyl)-carbamoyl]-2-decanoyl-amino-butyric acid benzyl ester was converted to 2-decanoylamino-4-({3-[2,5-diphenyl-oxazole-4-carbonyl]-1,2-phenyl}-carbamoyl)-butyric acid benzyl ester (113 mg, 64%) as a pale yellow solid: $^1$H NMR ($CDCl_3$) δ 8.36 (m, 1H), 7.95 (br, 2H), 7.42–7.15 (m, 16H), 6.67 (m, 1H), 5.03 (m, 2H), 4.58 (m, 1H), 2.47–1.89 (m, 6H), 1.50 (m, 2H), 1.09 (br, 12H), 0.86 (m, 3H).

**2-Decanoylamino-4-{{3-[2,5-diphenyl-oxazole-4-carbonyl)-1,2-phenyl}-carbamoyl)-butyric acid benzyl ester (FY8-αα09).** According to the procedure described for FY21-αα09, 2-decanoylamino-4-({3-[2,5-diphenyl-oxazole-4-carbonyl]-1,2-phenyl}-carbamoyl)-butyric acid benzyl ester was converted to FY8-αα09 (93.3 mg, 94%): $^1$H NMR ($CDCl_3$) δ 8.23 (m, 1H), 7.99 (m, 2H), 7.40–7.05 (m, 11H), 4.37 (m, 1H), 2.52–1.69 (m, 6H), 1.38 (m, 2H), 1.10 (br, 12H), 0.77 (m, 3H); MS (EI) *m*/*z* 638 ($M^+$), 620 ($[M-H_2O]^+$).

### FY9-αα09

**4-[(3-*t*-Butoxycarbonylamino-propyl)-carbamoyl]-2-decanoylamino-butyric acid benzyl ester.** According to the procedure described for **9**, **7** (304 mg, 0.776 mmol) was converted to 4-[(3-*t*-butoxycarbonylamino-propyl)-carbamoyl]-2-decanoylamino-butyric acid benzyl ester (279 mg, 66%): $^1$H NMR ($CDCl_3$) δ 7.36 (m, 5H), 6.72 (m, 1H), 5.16 (m, 2H), 4.56 (m, 1H), 3.29–3.11 (m, 4H), 2.27–2.15 (m, 4H), 1.99 (m, 1H), 1.73 (m, 2H), 1.63–1.57 (m, 3H), 1.44 (br, 9H), 1.26 (br, 12H), 0.88 (m, 3H).

**2-Decanoylamino-4-{{4-[2,5-diphenyl-oxazole-4-carbonyl]-propyl}-carbamoyl)-butyric acid benzyl ester.** According to the procedure described for **11**, 4-[(3-*t*-butoxycarbonylamino-propyl)-carbamoyl]-2-decanoylamino-butyric acid benzyl ester was converted to 2-decanoylamino-4-({4-[2,5-diphenyl-oxazole-4-carbonyl]-propyl}-carbamoyl)-butyric acid benzyl ester (131 mg, 63%): $^1$H NMR ($CDCl_3$) δ 8.37–7.33 (m, 15H), 6.79 (m, 2H), 5.16 (m, 2H), 4.58 (m, 1H), 3.53–3.32 (m, 4H), 2.32–2.17 (m, 6H), 1.87–1.73 (m, 4H), 1.23 (br, 12H), 0.86 (m, 3H).

**2-Decanoylamino-4-({4-[2,5-diphenyl-oxazole-4-carbonyl]-propyl}-carbamoyl)-butyric acid (FY9-αα09).** According to the procedure described for FY21-αα09, 2-decanoylamino-4-({4-[2,5-diphenyl-oxazole-4-carbonyl]-propyl}-carbamoyl)butyric acid benzyl ester was converted to FY9-αα09 (169 mg, quant.) as a pale yellow oil: $^1$H NMR ($CDCl_3$) δ 8.30–7.24 (m, 10H), 4.49 (m, 1H), 3.49–3.32 (m, 4H), 2.40 (m, 2H), 2.21 (m, 2H), 1.98 (m, 2H), 1.79 (m, 2H), 1.57 (m, 2H), 1.20 (br, 12H), 0.84 (m, 3H); MS (EI) *m*/*z* 604 ($M^+$), 586 ($[M-H_2O]^+$).

### FY10-αα09

**4-[(2-*t*-Butoxycarbonylamino-piperazine)-carbamoyl]-2-decanoyl-amino-butyric acid benzyl ester.** According to the procedure described for **9**, **7** (300 mg, 0.766 mmol) and *tert*-butyl 1-piperazinecarboxylate (143 mg, 0.768 mmol) were converted to 4-[(2-*t*-butoxycarbonylamino-piperazine)-carbamoyl]-2-decanoyl-amino-butyric acid benzyl ester (366 mg, 85%) as a yellow oil: $^1$H NMR ($CDCl_3$) δ 7.36 (br, 5H), 6.65 (m, 1H), 5.17 (m, 2H), 4.59 (m, 1H), 3.57 (m, 2H), 3.43 (m, 4H), 3.29 (m, 2H), 2.35–2.05 (m, 5H), 1.70 (m, 1H), 1.61 (m, 2H), 1.47 (br, 9H), 1.26 (br, 12H), 0.88 (m, 3H).

**2-Decanoylamino-4-{{3-[2,5-diphenyl-oxazole-4-carbonyl]-piperazine}-carbamoyl)-butyric acid benzyl ester.** According to the procedure described for **11**, 4-[(2-*t*-butoxycarbonylamino-piperazine)-carbamoyl]-2-decanoyl-amino-butyric acid benzyl ester was converted to 2-decanoylamino-4-({3-[2,5-diphenyl-oxazole-4-carbonyl]-piperazine}-carbamoyl)-butyric acid benzyl ester (160 mg, 68%): $^1$H NMR ($CDCl_3$) δ 8.10–7.29 (m, 15H), 6.65 (m, 1H), 5.14 (m, 2H), 4.60 (m, 1H), 3.78–3.34 (m, 8H), 2.38–2.08 (m, 5H), 1.86 (m, 1H), 1.59 (m, 2H), 1.24 (br, 12H), 0.86 (m, 3H).

**2-Decanoylamino-4-({3-[2,5-dlphenyl-oxazole-4-carbonyl-piperazine-carbamoyl)-butyric acid (FY10-αα09).** According to the procedure described for FY21-αα09, 2-decanoylamino-4-({3-[2,5-diphenyl-oxazole-4-carbonyl]-piperazine}-carbamoyl)-butyric acid benzyl ester was converted to FY10-αα09 (146 mg, quant.): $^1$H NMR ($CDCl_3$) δ 8.05–7.24 (m, 10H), 4.42 (m, 1H), 3.62–3.43 (m, 8H), 2.53 (m, 2H), 2.20 (m, 2H), 2.02 (m, 2H), 1.53 (m, 2H), 1.20 (br, 12H), 0.84 (m, 3H); MS (EI) *m*/z 616 ($M^+$), 598 ($[M-H_2O]^+$).

### SC-ααδ17A

**DL-2-(2,2,2-Trichloroethoxycarbonylamino)-pentanoic acid 5-allyl ester 1-methyl ester (2b).** To a stirred suspension of 5.0 g (34 mmol) of DL-glutamic acid (**1**) in 85 mL of allyl alcohol was added dropwise 10.8 mL (85 mmol) of chlorotrimethylsilane. The suspension was stirred at 22 °C for 13 h and concentrated in vacuo. The resulting oil was dissolved in 90 mL of dioxane. This solution was treated with 118.9 mmol of aqueous sodium carbonate (12.61 g in 90 mL of $H_2O$) at 0 °C, stirred for 5 min, and treated with 4.80 mL (34.7 mmol) of TrocCl. The reaction mixture was stirred at 0 °C for 10 min and warmed to 22 °C, stirred for 16 h, concentrated in vacuo, quenched with 150 mL of $H_2O$ and washed with $Et_2O$. The aqueous layer was acidified to pH 1 with concentrated HCl, salted out with NaCl, and extracted with EtOAc (3×). The resulting organic layer was dried ($Na_2SO_4$) and concentrated in vacuo to give

7.92 g of carboxylic acid as a yellow oil. To a solution of the resulting oil in 29 mL of DMF were added 3.50 g (35.0 mmol) of $KHCO_3$ and 1.60 mL (26.2 mmol) of iodomethane. The reaction mixture was stirred at 22 °C for 16 h, diluted with EtOAc, and washed with 10% HCl, $H_2O$, saturated aqueous $NaHCO_3$ and brine. The organic layer was dried ($Na_2SO_4$), concentrated in vacuo, and chromatographed on $SiO_2$ (hexanes:EtOAc, 5:1→4:1→3:1→2:1) to give 6.26 g (49% over three steps) of **2b** as a pale yellow oil: $^1$H NMR ($CDCl_3$) δ 5.95–5.86 (m, 1H), 5.71 (d, 1H, $J$ = 7.2 Hz), 5.34–5.22 (m, 2H), 4.74, 4.70 (AB, 2H, $J$ = 13.9 Hz), 4.58 (d, 2H, $J$ = 5.8 Hz), 4.47–4.40 (m, 1H), 3.77 (s, 3H), 2.50–2.42 (m, 2H), 2.32–2.23 (m, 1H), 2.07–2.00 (m, 1H); MS (CI) $m/z$ 376 ($[M+1]^+$).

**2-Oleoylamino-pentanedioic acid 5-allyl ester 1-methyl ester.** To a solution of 947 mg (2.51 mmol) of **2b** in 3.3 mL of acetic acid and 4.9 mL of THF was added 3.29 g (50.3 mmol) of zinc dust. The reaction mixture was stirred at 22 °C for 1 h, filtered through a Celite pad, and the filtrate was concentrated in vacuo. The resulting residue was diluted with EtOAc and washed with saturated aqueous $NaHCO_3$ and brine. The organic layer was dried ($Na_2SO_4$) and concentrated in vacuo to give free amine. This amine (67.7 mg) was dissolved in 1.1 mL of $CH_2CI_2$ and treated with 0.14 mL (1.02 mmol) of triethylamine and 0.17 mL (0.51 mmol) of oleoyl chloride at 0 °C. The reaction mixture was stirred at 0 °C for 15 min and warmed to 22 °C, stirred for 14 h, diluted with EtOAc, and washed with 10% HCl, $H_2O$, saturated aqueous $NaHCO_3$ and brine. The organic layer was dried ($Na_2$ $SO_4$), concentrated in vacuo, and chromatographed on $SiO_2$ (hexanes:EtOAc, 8:1→7:1→5:1) to give 110 mg (70%) of 2-oleoylamino-pentanedioic acid 5-allyl ester 1-methyl ester as a pale yellow oil: $^1$H NMR ($CDCl_3$) δ 6.12 (d, 1H, $J$ = 7.7 Hz), 5.98–5.85 (m, 1H), 5.37–5.23 (m, 4H), 4.68–4.58 (m, 3H), 3.76 (s, 3H), 2.47–2.17 (m, 6H), 2.07–1.95 (m, 4H), 1.60 (m, 2H), 1.30 (brd, 20H), 0.89 (m, 3H); MS (EI) $m/z$ 465 ($M^+$).

**4-[(2-Allyloxycarbonylamino-ethyl)-benzyl-carbamoyl]-2-oleoyl-amino-butyric acid methyl ester.** To a solution of 110 mg (0.236 mmol) of 2-oleoylamino-pentanedioic acid 5-allyl ester 1-methyl ester in 1 mL of THF was added 0.20 mL (2.4 mmol) of morpholine followed by 27.3 mg (0.024 mmol) of tetrakistriphenylphosphine Pd(0) under nitrogen atmosphere at 22 °C. After stirring for 30 min, the reaction mixture was diluted with EtOAc, and washed with 10% HCl and brine. The organic layer was dried ($Na_2SO_4$) and concentrated in vacuo. The resulting residue and 27.0 mg (0.115 mmol) of diamine segment were dissolved in 0.5 mL of THF. The solution was treated with 0.03 mL (0.18 mmol) of *N,N*-diisopropylethylamine and 0.070 g (0.15 mmol) of PyBroP at 0 °C, stirred for 1 h, warmed to 22 °C and stirred for 9 h. The reaction mixture was diluted with EtOAc, washed with 10% HCl, $H_2O$, saturated aqueous $NaHCO_3$ and brine. The organic layer was dried ($Na_2SO_4$), concentrated in vacuo, and chromatographed on $SiO_2$ (hexanes:EtOAc, 1:1→1:2) to give 169 mg (quant.) of 4-[(2-allyloxycarbonylamino-ethyl)-benzyl-carbamoyl]-2-oleoyl-amino-butyric acid methyl ester: $^1$H NMR ($CDCl_3$) δ 7.69–7.13 (m, 5H), 6.65 (m, 1H), 5.91–5.85 (m, 2H), 5.35–5.17 (m, 4H), 4.61–4.45 (m, 5H), 3.73–3.36 (m, 7H), 2.45–2.00 (m, 10H), 1.60 (m, 2H), 1.27 (br, 20H), 0.86 (m, 3H); MS (EI) $m/z$ 641 ($M^+$).

**2-Oleoylamino-4-(benzyl-{3-[2,5-diphenyl-oxazole-4-carbonyl]-ethyl}-carbamoyl)-butyric acid methyl ester.** To a solution of 169 mg (0.263 mmol) of 4-[(2-allyloxycarbonylamino-ethyl)-benzyl-carbamoyl]-2-oleoyl-amino-butyric acid methyl ester in 2 mL of $CH_2Cl_2$ were added 0.031 mL (0.53 mmol) of acetic acid and 9 mg (0.008 mmol) of tetrakistriphenylphosphine Pd(0) followed by 0.092 mL (0.34 mmol) of tributyltin hydride under nitrogen atmosphere at 22 °C. After stirring for 30 min, the reaction mixture was diluted with EtOAc and washed with saturated aqueous $NaHCO_3$ and brine. The organic layer was dried ($Na_2SO_4$) and concentrated in vacuo. The resulting residue and 70 mg (0.26 mmol) of oxazole segment **10** were dissolved in 1 mL of THF. To this solution was added 0.092 mL (0.66 mmol) of triethylamine followed by 0.221 g (0.473 mmol) of PyBroP at 0 °C. After stirring at 0 °C for 1 h and at 22 °C for 12 h, the reaction mixture was diluted with EtOAc and washed with 10% HCl, $H_2O$, saturated aqueous $NaHCO_3$ and brine. The organic layer was dried ($Na_2SO_4$), concentrated in vacuo, and chromatographed on $SiO_2$ (hexane:EtOAc, 2:1→1:1) to give 2-oleoylamino-4-(benzyl-{3-[2,5-diphenyl-oxazole-4-carbonyl]-ethyl}-carbamoyl)-butyric acid methyl ester (104 mg, 55%) as a pale yellow oil: $^1$H NMR ($CDCl_3$) δ 8.37–8.35 (m, 2H), 8.10 (m, 2H), 7.52–7.13 (m, 6H), 5.31 (m, 2H), 4.70–4.60 (m, 3H), 3.68–3.52 (m, 7H), 2.13–1.95 (m, 10H), 1.64 (m, 2H), 1.26 (br, 20H), 0.90 (m, 3H); MS (EI) $m/z$ 804 ($M^+$).

**2-Oleoylamino-4-(benzyl-{3-[2,5-diphenyl-oxazole-4-carbonyl]-ethyl}-carbamoyl)-butyric acid (SC-ααδ17A).** To a solution of 104 mg (0.129 mmol) of 2-oleoylamino-4-(benzyl-{3-[2,5-diphenyl-oxazole-4-carbonyl]-ethyl}-carbamoyl)-butyric acid methyl ester in 0.5 mL of dioxane was added 1.6 mmol of aqueous lithium hydroxide (65 mg in 0.2 mL of $H_2O$) at 0 °C. The reaction mixture was stirred at 0 °C for 10 min and at 22 °C for 1 h, poured into 50 mL of $H_2O$ and washed with $Et_2O$. The aqueous layer was acidified to pH 1 with 10% HCl, salted out with NaCl, and extracted with EtOAc (3×). The resulting organic layer was dried ($Na_2SO_4$) and concentrated in vacuo to give SC-αaδ17A (28.1 mg, 28%) as a pale yellow oil: $^1$H NMR ($CDCl_3$) δ 8.26–8.23 (m, 2H), 8.01 (m, 2H), 7.43–7.07 (m, 11H), 5.25 (m, 2H), 4.69–4.49 (m, 2H), 4.34–4.26 (m, 1H), 3.82–3.45 (m, 6H), 2.19–1.91 (m, 8H), 1.47 (m, 2H), 1.18 (br, 20H), 0.80 (m, 3H); HRMS (EI) $m/z$ calcd for $C_{48}H_{60}N_4O_5$ ($[M-H_2O]^+$): 772.4564; found: 772.4540.

## SC-ααδ17B

**4-[(2-Allyloxycarbonylamino-ethyl)-benzyl-carbamoyl]-2-(2,2,2-trichloroethoxycarbonylamlno)-butyric acid methyl ester (3).** According to the procedure described for 4-[(2-allyloxycarbonylamino-ethyl)-benzyl-carbamoyl]-2-

oleoyl-amino-butyric acid methyl ester, **2b** (217 mg, 0.577 mmol) was converted to 4-[(2-allyloxycarbonyl-amino-ethyl)-benzyl-carbamoyl]-2-(2,2,2-trichloroethoxycarbonyl-amino)-butyric acid methyl ester (**3**, 294 mg, 92%) as an orange oil: $^1$H NMR ($CDCl_3$) δ 7.68–7.11 (m, 5H), 6.08 (m, 1H), 5.91 (m, 1H), 5.32–5.19 (m, 2H), 4.8 1–4.40 (m, 5H), 3.80–3.65 (m, 5H), 3.40 (m, 2H), 2.61–2.31 (m, 6H); MS (EI) *m*/*z* 553 ($M^+$).

**2-(2,2,2-Trichloroethoxycarbonylamino)-4-(benzyl-{3-[2,5-diphenyl-oxazole-4-carbonyl]-ethyl}-carbamoyl)-butyric acid methyl ester (4).** According to the procedure described for 2-oleoylamino-4-(benzyl-{3-[2,5-diphenyl-oxazole-4-carbonyl]-ethyl}-carbamoyl)-butyric acid methyl ester, 4-[(2-allyloxycarbonylamino-ethyl)-benzyl-carbamoyl]-2-(2,2,2-trichloroethoxycarbonyl-amino)-butyric acid methyl ester (**3**, 887 mg, 1.604 mmol) was converted to 2-(2,2,2-trichloroethoxy-carbonylamino)-4-(benzyl-{3-[2,5-diphenyl-oxazole-4-carbonyl]-ethyl}-carbamoyl)-butyric acid methyl ester (**4**, 819 mg, 71%) as a pale yellow oil: $^1$H NMR ($CDCl_3$) δ 8.38–8.35 (m, 2H), 8.13–8.09 (m, 2H), 7.53–7.13 (m, 11H), 4.74–4.58 (m, 4H), 4.36 (m, 1H), 3.80–3.52 (m, 7H), 2.51–2.05 (m, 4H); MS (EI) *m*/*z* 716 ($M^+$).

**2-Linoleylamino-4-(benzyl-{3-[2,5-diphenyl-oxazole-4-carbonyl]-ethyl}-carbamoyl)-butyric acid methyl ester.** To a solution of 143 mg (0.199 mmol) of 2-(2,2,2-trichloroethoxycarbonylamino)-4-(benzyl-{3-[2,5-diphenyl-oxazole-4-carbonyl]-ethyl}-carbamoyl)-butyric acid methyl ester in 0.3 mL of acetic acid and 0.5 mL of THF was added 0.260 g (3.98 mmol) of zinc dust. The reaction was stirred at 22 °C for 1 h. The mixture was filtered through a Celite pad and the filtrate was concentrated in vacuo. The resulting residue was diluted with EtOAc and washed with saturated aqueous $NaHCO_3$ and brine. The organic layer was dried ($Na_2SO_4$) and concentrated in vacuo to give free amine. The resulting residue was dissolved in 0.1 mL of $CH_2Cl_2$ and treated with 0.3 mg (0.003 mmol) of DMAP, 9.3 μl (0.03 mmol) of linoleic acid and 6.2 mg (0.032 mmol) of EDCI at 0 °C. The reaction mixture was stirred at 0 °C for 15 min and warmed to 22 °C, stirred for 14 h, diluted with EtOAc, and washed with 10% HCl, $H_2O$, saturated aqueous $NaHCO_3$ and brine. The organic layer was dried ($Na_2SO_4$), concentrated in vacuo, and chromatographed on $SiO_2$ (hexanes:EtOAc, 7:1→5:1) to give 67.7 mg (42%) of 2-linoleylamino-4-(benzyl-{3-[2,5-diphenyl-oxazole-4-carbonyl]-ethyl}-carbamoyl)-butyric acid methyl ester of as a colorless oil: $^1$H NMR ($CDCl_3$) δ 8.37–8.35 (m, 2H), 8.13–8.07 (m, 2H), 7.52–7.13 (m, 11H), 5.33 (m, 4H), 4.70–4.51 (m, 3H), 3.75–3.52 (m, 7H), 2.76 (m, 2H), 2.45 (m, 2H), 2.23–1.99 (m, 8H), 1.55 (m, 2H), 1.26 (br, 14H), 0.88 (m, 3H); MS (EI) *m*/*z* 802 ($M^+$).

**2-Linoleylamino-4-(benzyl-{3-[2,5-diphenyl-oxazole-4-carbonyl]-ethyl}-carbamoyl)-butyric acid (SC-ααδ17B).** According to the procedure described for SCααδ17A, 2-linoleylamino-4-(benzyl-{3-[2,5-diphenyl-oxazole-4-carbonyl]-ethyl}-carbamoyl)-butyric acid methyl ester (67.7 mg, 0.0843 mmol) was converted to SC-ααδ17B (66.4 mg, 99%) as a pale yellow oil: $^1$H NMR ($CDCl_3$) δ 8.33–8.30 (m, 2H), 8.08 (m, 2H), 7.50–7.03 (m, 11H), 5.34 (m, 2H), 4.72–4.42 (m, 4H), 4.13–4.07 (m, 1H), 3.80–3.48 (m, 4H), 2.75 (m, 2H), 2.50–2.01 (m, 10H), 1.54 (m, 2H), 1.23 (br, 14H), 0.88 (m, 3H); HRMS (EI) *m*/*z* calcd for $C_{48}H_{59}N_4O_5$ (M–OH): 771.4485; found: 771.4487.

## SC-ααδA

**2-Citronellylamino-pentanedioic acid 5-allyl ester 1-methyl ester.** To a solution of 947 mg (2.51 mmol) of **2b** in 3.3 mL of acetic acid and 4.9 mL of THF was added 3.286 g (50.27 mmol) of zinc dust. The reaction was stirred at 22 °C for 1 h. The mixture was filtered through a Celite pad and the filtrate was concentrated in vacuo. The resulting residue was diluted with EtOAc and washed with saturated aqueous $NaHCO_3$ and brine. The organic layer was dried ($Na_2SO_4$) and concentrated in vacuo to give free amine. The resulting residue (68.7 mg) was dissolved in 1.1 mL of $CH_2Cl_2$ and treated with 4.2 mg (0.034 mmol) of DMAP, 69 μL (0.38 mmol) of racemic citronellic acid and 79 mg (0.41 mmol) of EDCI at 0 °C. The reaction mixture was stirred at 0 °C for 15 min and warmed to 22 °C, stirred for 14 h, diluted with EtOAc, and washed with 10% HCl, $H_2O$, saturated aqueous $NaHCO_3$ and brine. The organic layer was dried ($Na_2SO_4$), concentrated in vacuo, and chromatographed on $SiO_2$ (hexanes:EtOAc, 7:1→5:1) to give 83.9 mg (69%) of 2-citronellylamino-pentanedioic acid 5-allyl ester 1-methyl ester as a colorless oil: $^1$H NMR ($CDCl_3$) δ 6.19 (d, 1H, $J$ = 7.4 Hz), 5.95–5.86 (m, 1H), 5.34–5.23 (m, 2H), 5.09 (m, 1H), 4.66–4.57 (m, 3H), 3.75 (s, 3H), 2.48–1.97 (m, 9H), 1.68 (s, 3H), 1.60 (s, 3H), 1.38–1.36 (m, 1H), 1.26–1.20 (m, 1H), 0.99–0.93 (m, 3H); MS (EI) *m*/*z* 353 ($M^+$).

**4-[(2-Allyloxycarbonylamino-ethyl)-benzyl-carbamoyl]-2-citronellyl-amino-butyric acid methyl ester.** According to the procedure described for 4-[(2-allyloxycarbonyl-amino-ethyl)-benzyl-carbamoyl]-2-oleoyl-amino-butyric acid methyl ester, 2-citronellylamino-pentanedioic acid 5-allyl ester 1-methyl ester (83.9 mg, 0.237 mmol) was converted to 4-[(2-allyloxycarbonylamino-ethyl)-benzyl-carbamoyl]-2-citronellyl-amino-butyric acid methyl ester (128 mg, quant.) as a brown oil: $^1$H NMR ($CDCl_3$) δ 7.70–7.13 (m, 5H), 6.56 (m, 1H), 5.92–5.86 (m, 1H), 5.72 (br, 1H), 5.32–5.18 (m, 2H), 5.08 (m, 1H), 4.62–4.45 (m, 5H), 3.74–3.71 (m, 5H), 3.42–3.23 (m, 4H), 2.50–1.93 (m, 9H), 1.67 (s, 3H), 1.59 (s, 3H), 1.37–1.32 (m, 1H), 1.26–1.18 (m, 1H), 0.92 (m, 3H); MS (FAB) *m*/*z* 530 ($[M+1]^+$).

**2-Citronellylamino-4-(benzyl-{3-[2,5-diphenyl-oxazole-4-carbonyl]-ethyl}-carbamoyl)-butyric acid methyl ester.** According to the procedure described for 2-oleoyl-amino-4-(benzyl-{3-[2,5-diphenyl-oxazole-4-carbonyl]-ethyl}-carbamoyl)-butyric acid methyl ester, 4-[(2-allyl-oxycarbonylamino-ethyl)-benzyl-carbamoyl]-2-citronellyl-amino-butyric acid methyl ester (128 mg, 0.241 mmol) was converted to 2-citronellylamino-4-(benzyl-{3-[2,5-diphenyl-oxazole-4-carbonyl]-ethyl}-carbamoyl)-butyric acid methyl ester (152 mg, 92%) as a pale yellow oil: $^1$H NMR ($CDCl_3$) δ 8.37 (m, 2H), 8.10 (m, 2H),

7.69–7.15 (m, 11H), 5.04 (m, 1H), 4.69–4.60 (m, 3H), 3.68–3.52 (m, 7H), 2.48–1.86 (m, 9H), 1.65 (s, 3H), 1.57 (s, 3H), 1.28–1.26 (m, 2H), 0.85 (m, 3H); MS (EI) *m*/*z* 692 ($M^+$).

**2-Citronellylamino-4-(benzyl-{3-[2,5-diphenyl-oxazole-4-carbonyl)-ethyl}-carbamoyl)-butyric acid (SC-ααδA).** According to the procedure described for SCααδ17A, 2-citronellylamino-4-(benzyl-{3-[2,5-diphenyl-oxazole-4-carbonyl]-ethyl}-carbamoyl)-butyric acid methyl ester (152 mg, 0.219 mmol) was converted to SC-ααδA (87.1 mg, 58%): $^1$H NMR ($CDCl_3$) δ 8.29 (m, 2H), 8.08 (m, 2H), 7.50–7.13 (m, 11H), 5.03 (m, 1H), 4.72–4.37 (m, 3H), 3.78–3.56 (m, 4H), 2.78–1.91 (m, 9H), 1.56 (s, 3H), 1.54 (s, 3H), 1.28–1.14 (m, 2H), 0.87 (m, 3H); HRMS (EI) *m*/*z* calcd for $C_{40}H_{46}N_4O_6$: 678.3417; found: 678.3441.

## SC-αaδ4II

**2-[2-(2-Methoxyethoxy)acetyl]-amino-4-(benzyl-{3-[2,5-diphenyl-oxazole-4-carbonyl]-ethyl}-carbamoyl)-butyric acid methyl ester (5).** To a solution of 290 mg (0.404 mmol) of 2-(2,2,2-trichloroethoxycarbonylamino)-4-(benzyl-{3-[2,5-diphenyl-oxazole-4-carbonyl]-ethyl}-carbamoyl)-butyric acid methyl ester (**4**) in 0.53 mL of acetic acid and 0.79 mL of THF was added 529 mg (8.09 mmol) of zinc dust. The reaction was stirred at 22 °C for 1 h. The mixture was filtered through a Celite pad and the filtrate was concentrated in vacuo. The resulting residue was diluted with EtOAc and washed with saturated aqueous $NaHCO_3$ and brine. The organic layer was dried ($Na_2SO_4$) and concentrated in vacuo to give free amine. This amine (112 mg) was dissolved in 0.7 mL of THF and treated with 72 μL (0.52 mmol) of triethylamine, 26 μl (0.23 mmol) of 2-(2-methoxyethoxy)-acetic acid and 173 mg (0.372 mmol) of PyBroP at 0 °C. The reaction mixture was stirred at 0 °C for 1 h and warmed to 22 °C, stirred for 11 h, diluted with EtOAc, and washed with 10% HCl, $H_2O$, saturated aqueous $NaHCO_3$ and brine. The organic layer was dried ($Na_2SO_4$), concentrated in vacuo, and chromatographed on $SiO_2$ (hexanes:EtOAc, 1:1→1:4→1:5→EtOAc only) to give 68.2 mg (50%) of **5**: $^1$H NMR ($CDCl_3$) δ 8.36 (m, 2H), 8.11 (m, 2H), 7.52–7.13 (m, 11H), 4.69–4.60 (m, 3H), 4.00 (m, 2H), 3.68–3.47 (m, 11H), 3.35 (s, 3H), 2.48–1.83 (m, 4H); HRMS (EI) *m*/*z* calcd for $C_{36}H_{40}N_4O_8$: 656.2846; found: 656.2844.

**2-[2-(2-Methoxyethoxy)acetyl]-amino-4-(benzyl-{3-[2,5-diphenyl-oxazole-4-carbonyl]-ethyl}-carbamoyl)-butyric acid (SC-αaδ4II).** According to the procedure described for SC-ααδ17A, 2-[2-(2-methoxyethoxy)acetyl]-amino-4-(benzyl-{3-[2,5-diphenyl-oxazole-4-carbonyl]-ethyl}-carbamoyl)-butyric acid methyl ester (**6**, 68.2 mg, 0.104 mmol) was converted to SC-ααδ4II (70.3 mg, quant.) as a pale yellow oil: $^1$H NMR ($CDCl_3$) δ 9.28 (brs, 1H), 8.21 (m, 2H), 7.99 (m, 2H), 7.39–7.05 (m, 11H), 4.63–4.46 (m, 3H), 3.90 (m, 2H), 3.61–3.42 (m, 8H), 3.24 (s, 3H), 2.63–1.96 (m, 4H); HRMS (EI) *m*/*z* calcd for $C_{35}H_{38}N_4O_8$: 642.2690; found: 642.2702.

## SC-αaδ6III

**2-2-[2-(2-Methoxyethoxy)ethoxy]acetyl}-amino-4-(benzyl-{3-[2,5-diphenyl-oxazole-4-carbonyl]-ethyl}-carbamoyl)-butyric acid methyl ester (6).** According to the procedure described for 2-[2-(2-methoxyethoxy)acetyl]-amino-4-(benzyl-{3-[2,5-diphenyl-oxazole-4-carbonyl]-ethyl}-carbamoyl)-butyric acid methyl ester (**5**), 2-(2,2,2-trichloroethoxycarbonylamino)-4-(benzyl-{3-[2,5-diphenyl-oxazole-4-carbonyl]-ethyl}-carbamoyl)-butyric acid methyl ester (**4**) was converted to 2-{2-[2-(2-methoxyethoxy)ethoxy]acetyl}-amino-4-(benzyl-{3-[2,5-diphenyl-oxazole-4-carbonyl]-ethyl}-carbamoyl)-butyric acid methyl ester (**6**, 57.2 mg, 39%): $^1$H NMR ($CDCl_3$) δ 8.37 (m, 2H), 8.11 (m, 2H), 7.51–7.13 (m, 11H), 4.73–4.60 (m, 3H), 3.98 (m, 2H), 3.71–3.50 (m, 15H), 3.33 (s, 3H), 2.50–2.02 (m, 4H); MS (EI) *m*/*z* 700 ($M^+$).

**2-{2-[2-(2-Methoxyethoxy)ethoxy]acetyl}-amino-4-(benzyl-{3-[2,5-diphenyl-oxazole-4-carbonyl-ethyl}-carbamoyl)-butyric acid (SC-ααδ6III).** According to the procedure described for SC-ααδ17A, **6** (57.2 mg, 0.0816 mmol) was converted to SC-ααδ6III (52.9 mg, 94%) as a pale yellow oil: $^1$H NMR ($CDCl_3$) δ 8.80 (brs, 1H), 8.24 (m, 2H), 8.01 (m, 2H), 7.42–7.06 (m, 11H), 4.65–4.45 (m, 3H), 3.90 (m, 2H), 3.63–3.43 (m, 12H), 3.26 (s, 3H), 2.90–2.20 (m, 4H); HRMS (EI) *m*/*z* calcd for $C_{37}H_{42}N_4O_9$: 686.2952; found: 686.2958.

## Plasmids and reagents

Plasmids pGEX2T-KG containing the GST-fusion of full length human $Cdc25B_2$ were previously described.[1] Recombinant human PTP1B was a gift from Dr. Zhong-Yin Zhang (Albert Einstein College of Medicine, Bronx, NY). To generate recombinant human VHR, we excised the coding sequence for VHR phosphatase from pT7-7-VHR (a gift from Dr. Jack E. Dixon, University of Michigan, Ann Arbor, MI) using Ned and EcoRI. The resulting DNA was ligated into the pMTL 22 vector. The pMTL 22-VHR plasmid was used to transform *DH5α Escherichia coli,* and the plasmid DNA was purified. The VHR phosphatase sequence from pMTL 22-VHR was excised with EcoRV and XhoI and ligated into the pGEX-4T3 plasmid, which had been digested with SmaI and XhoI. The pGEX-4T3 plasmids were used to transform *DH5α E. coli*. This clone was then used to produce the GST-VHR phosphatase protein as were all other recombinant fusion proteins by our previously published methods.[1]

## Tyrosine specific phosphatase and dual specificity phosphatase assays

The activity of the GST-tagged dual specificity phosphatases and recombinant tyrosine specific phosphatase was measured in 96-well microtiter plates with *O*-methylfluorescein monophosphate (OMFP) (Sigma, St. Louis, MO) as the substrate in three to six independent experiments. The phosphatases catalyzed the metabolism of OMFP to the fluorescent product *O*-methylfluorescein

(OMF) (Sigma; St. Louis, MO). The reaction mixture (150 μL) consisted of 30 mM Tris (pH 7.0), 75 mM NaCl, 1 mM EDTA, 0.033% bovine serum albumin and 1 mM DTT for GST-VHR and rhPTP1B or 30 mM Tris (pH 8.0), 75 mM NaCl, 1 mM EDTA, 0.033% bovine serum albumin and 1 mM DTT for GST-$Cdc25B_2$. Substrate concentrations approximating the $K_m$ were used: VHR, 10 μM; rhPTP1B, 200 μM; $Cdc25B_2$, 40 μM. Both the substrate and compounds were resuspended in DMSO and diluted in water; the final DMSO concentration remained at 7% for all assays. The inhibitory potential for each compound was monitored at 0, 3 and 100 μM reaction concentrations, and the reactions were initiated by the addition of ~0.025 μg of VHR, ~0.25 μg of rhPTP1B and ~0.10 μg $Cdc25B_2$. Reaction length varied with each phosphatase: 21 min for GST-VHR, 14 min for rhPTP1B and 60 min for $Cdc25B_2$. Fluorescent emissions from the hydrolysis of OMFP to OMF were measured at 25 °C during the entire course of the reaction using a Perseptive Biosystems Cytofluor II (Framingham, MA) with an excitation filter of 485 nm (20 nm band width) and an emissions filter of 530 nm (30 nm band width). The fluorescent emissions were converted to units of product formation using an OMF standard curve that was performed with each experiment. Spontaneous hydrolysis of OMFP to OMF as monitored in an enzyme free reaction was normalized to the OMF standard curve. Product formation with 0 μM inhibitor was also monitored and determined to be linear for all enzymes over the incubation period. Furthermore, the reaction was directly proportional to both the enzyme and substrate concentration.

### Steady-state kinetics

Initial enzyme rates with five to eight inhibitor concentrations were determined using at least eight substrate (OMFP) concentrations between $K_m/2$ and $5^*K_m$. The $V_0$ for each substrate concentration was determined and then fit to the Michaelis–Menten equation as previously described[1] using GraphPad Prism 3.0 (GraphPad Software, Inc., San Diego, CA). The best fit kinetic model and inhibition constants were obtained using EZ-Fit™ (Perrella Scientific, Amherst, NH).

### Determination of clog *P* values

Computation of clog *P*, the calculated logarithm of the octanol–water partition coefficient, was performed on an Indigo2 R4400 workstation according to a previously published protocol.[26] Extended conformations of compounds were fully optimized using the semi-empirical method PM3. Charges and other parameters for the regression analysis were also obtained with the PM3 module on Spartan 5.0 (Wavefunction, Inc., Irvine, CA).

### Cell culture and anti-proliferation studies

We used human MDA-MB-231 and MCF-7 breast cancer cells to determine the antiproliferative activity of several compounds.[19] Cells were plated at 2000 cells per well in RPMI-1640 culture medium containing 10% fetal bovine serum. After a 24 h incubation, 100 μM of selected compounds were added to the cells. The cells were then incubated with the compounds for 72 h and viable cell number was determined by our previously described method using 3-[4,5-dimethylthiazol-2-yl]-2,5-diphenyl tetrazolium bromide.[19] All results were normalized to vehicle treated control values.

For cell cycle studies, we used the previously described tsFT210 cells.[27] Cells were plated at $2\times10^5$ cells/mL and maintained at 32.0 °C until they were blocked at $G_2$ phase by incubation at 39.4 °C for 17 h. The synchronized cells were then released from $G_2$ blockage by reincubating at 32.0 °C and treated immediately with FY21-αα09, SC-ααδ9, nocodazole or the DMSO vehicle to probe for $G_2$/M arrest. After a 6 h incubation, cells were harvested with phosphate buffered saline and stained with a solution containing 50 μg/mL propidium iodide and 250 μg/mL RNase A. Flow cytometry analyses were conducted with a Becton Dickinson FACS Star (Becton Dickinson, Franklin Lakes, NJ).

### Acknowledgements

We are grateful for the helpful molecular biology advice of Dr. Iliya Lefterov, the cell culture results of Angela Wang and the excellent technical assistance of Eileen Southwick. This work was supported in part by Army Breast Cancer Predoctoral Research Fellowship DAMDI7-94-J4193 and Grant DAMD17-97-1-7229, the Fiske Drug Discovery Fund, and USPHS NIH Grants CA 78039 and GM 55433.

### References and Notes

1. Rice, R. L.; Rusnak, J. M.; Yokokawa, F.; Yokokawa, S.; Messner, D. J.; Boynton, A. L.; Wipf, P.; Lazo, J. S. *Biochemistry* **1997**, *36*, 15965.
2. Tonks, N. K.; Neel, B. G. *Cell* **1996**, *87*, 365.
3. Hunter, T. *Cell* **1995**, *80*, 225.
4. Taing, M.; Keng, Y.-F.; Shen, K.; Wu, L.; Lawrence, D. S.; Zhang, Z.-Y. *Biochemistry* **1999**, *38*, 3793.
5. Denu, J. M.; Stuckey, J. A.; Saper, M. A.; Dixon, J. E. *Cell* **1996**, *87*, 361.
6. Flint, A. J.; Tigianis, T.; Barford, D.; Tonks, N. K. *Proc. Natl. Acad. Sci. USA* **1997**, *94*, 1680.
7. Stone, R. L.; Dixon, J. E. *J. Biol. Chem.* **1994**, *269*, 31323.
8. Brown-Shimer, S.; Johnson, K. A.; Hill, D. E.; Bruskun, A. M. *Cancer Res.* **1992**, *52*, 478.
9. Li, L.; Ernsting, B. R.; Wishart, M. J.; Lohse, D. L.; Dixon, J. E. *J. Biol. Chem.* **1997**, *272*, 29403.
10. Seely, B. L.; Staubs, P. A.; Reichart, D. R.; Berhanu, P.; Milarski, K. L.; Saltiel, A. R.; Kusari, J.; Olefsky, J. M. *Diabetes* **1996**, *45*, 1379.
11. Liu, F.; Hill, D. E.; Chernoff, J. *J. Biol. Chem.* **1996**, *271*, 31290.
12. Todd, J. L.; Tanner, K. G.; Denu, J. M. *J. Biol. Chem.* **1999**, *274*, 13271.
13. Yuvaniyama, J.; Denu, J. M.; Dixon, J. E.; Saper, M. A. *Science* **1996**, *272*, 1328.
14. Fauman, E. B.; Cogswell, J. P.; Lovejoy, B.; Rocque, W. J.; Holmes, W.; Montana, V. G.; Piwnica-Worms, H.; Rink, M. J.; Saper, M. A. *Cell* **1998**, *93*, 617.

15. Baldin, V.; Cans, C.; Superti-Furga, G.; Ducommun, B. *Oncogene* **1997**, *14*, 2485.
16. Gabrielli, B. G.; De Souza, C. P.; Tonks, I. D.; Clark, J. M.; Hayward, N. K.; Ellem, A. *J. Cell. Sci.* **1996**, *109*, 1081.
17. Gabrielli, B. G.; Clark, J. M.; McCormack, A. K.; Ellem, K. A. *J. Biol. Chem.* **1997**, *272*, 28607.
18. Stuckey, J. A.; Schubert, H. L.; Fauman, E. B.; Zhang, Z.-Y.; Dixon, J. E.; Saper, M. A. *Nature* **1994**, *370*, 571.
19. Wipf, P.; Cunningham, A.; Rice, R. L.; Lazo, J. S. *Bioorg. Med. Chem.* **1997**, *5*, 165.
20. Bergnes, G.; Gilliam, C. L.; Boisclair, M. D.; Blanchard, J. L.; Blake, K. V.; Epstein, D. M.; Pal, K. *Bioorg. Med. Chem. Lett.* **1999**, *9*, 2843.
21. Puius, Y. A.; Zhao, Y.; Sullivan, M.; Lawrence, D. S.; Almo, S. C.; Zhang, Z.-Y. *Proc. Natl. Acad. Sci. USA* **1997**, *94*, 13420.
22. Tamura, K.; Rice, R. L.; Wipf, P.; Lazo, J. S. *Oncogene* **1999**, *18*, 6989.
23. Gunasekera, S. P.; McCarthy, P. J.; Kelly-Borges, M. *J. Am. Chem. Soc.* **1996**, *118*, 8759.
24. Blanchard, J. L.; Epstein, D. M.; Boisclair, M. D.; Rudolph, J.; Pal, K. *Bioorg. Med. Chem. Lett.* **1999**, *9*, 2537.
25. Peng, H.; Zalkow, L. H. *J. Med. Chem.* **1998**, *41*, 4677.
26. Alkorta, I.; Villar, H. O. *Int. J. Quant. Chem.* **1992**, *44*, 203.
27. Th'ng, J. P.; Wright, P. S.; Hamaguchi, J.; Lee, M. G.; Norbury, C. J.; Nurse, P.; Bradbury, E. M. *Cell* **1990**, *63*, 313.